Measurement of interface deformation and magnetic field distribution at a conducting two-fluid system [1] [2] [3]

Carsten Sievert

Diploma Thesis
TU Ilmenau, Fakultät Elektro- und Informationstechnik
September 24, 2004

[1] Diplomarbeit im Studiengang Elektro- und Informationstechnik, 2346-04D-01
[2] Betreuender Hochschullehrer: Prof. Andre Thess
[3] Betreuer: Dr. Christian Resagk

Contents

Chapter 1

Introduction

1.1 The experiment

The experiment described here is part of the B-1 project of the DFG research group on MHD at TU Ilmenau. The B-1 and B-2 project aim at interface reconstruction by magnetic field measurements.
The central part of the experimental apparatus is a transparent cylindrical container, with 9.5 cm height and 5 cm inner diameter, that is filled with Galinstan and an electrolyte. Due to the different densities and the fact that the two liquids do not mix, the Galinstan is located in the lower part of the cylinder and an interface dividing the fluids can be observed both from above and the sides. Externally excited vibrations cause the fluid interface to deform, often by stable oscillations if the exciting frequency is chosen accordingly.
Through the fluids, a DC current is passed vertically. Without any interface deformation, this current will have a homogenous current density distribution inside the cylinder and create a radial-symmetric magnetic field with only an azimuthal component. In the case of a disturbed interface, the current will choose a way of minimal ohmic resistance, therefore giving high current densities at Galinstan crests and low densities at hollows. Because of these changes of the current distribution and the fact that the current leaves the metal perpendicular to its surface, there is a change of the current's magnetic field (distribution and orientation), which is observed by a ring of sensors outside the cylinder.
The key point of the experiment is the possibility to observe the periodic changes of the interface shape by optical and electromagnetic means, which are physically completely separated.

1.2 Motivation

In many technological or scientific tasks, it is necessary or desirable to have information on the internal structure of some system, as the distribution of different materials within. Still, this information may be difficult to obtain, because the system does not allow visual observation and other methods as invasive (destructive), ultrasonic or X-ray cannot be applied. For certain cases, inverse field theory allow-

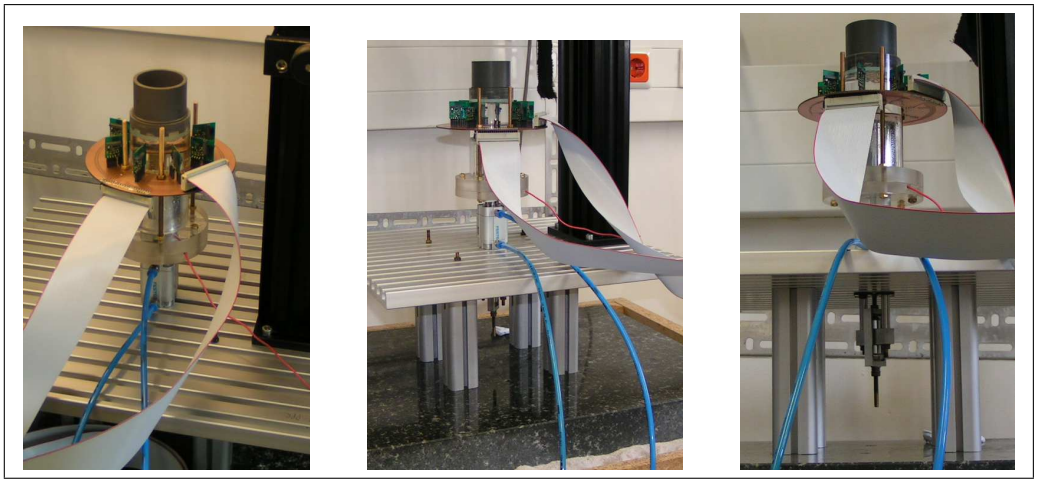

Figure 1.1: The experiment: one can see the cylinder, the sensor ring and flat cables, the pneumatic shaker and the amplitude control below the base plate

ing to recalculate a current distribution from a given (i.e. measured) magnetic field may be an appropriate solution, if the system's internal structure can be related to different electrical conductivities. Of course this implies, that an electrical current can be passed through the system or even is one of the fundamental properties of the system.
This is the case in aluminium reduction, from which our experiment is derived.
Here, molten and highly conducting aluminium is found below a layer of aluminium oxide (Al_2O_3) and cryolite ($Na_3[AlF_6]$), and a current is vertically passed through the system. The interest in the fluid-fluid-interface in this task is caused by the fact, that the interface is not always stable, but may show strong wave motion ([Davidson]). This wave motion can destroy parts of the processing unit and needs to be controlled.
Other similar applications found in the literature ([ThomäSievert04]) are quality check of fuel cells, medical applications and geophysics. But it must be noticed, that unlike the case of aluminium electrolysis most of these tasks do not include movement of the interface, making them somewhat more simple and limiting the need for quick algorithms.

1.3 Previous works

In 1999, Kevin Hope investigated the behavior of one and two fluid systems [Hope99]. The system contained water and/or Galinstan and was subjected to mechanical oscillations. He reports good results in the observations of the systems by means of PIV. It is interesting that he reports the amplitudes of internal waves to be rather strong, if the system has got a fixed top.
The Projektarbeit "Measurement of Faraday-Oscillations at the interface of two fluids" by Dietmar Link [Link02] treated the Theory of Faraday Oscillations and describes measurements with the electromagnetic shaker and observed mode shapes

and spectra of vibrations.
Another Projektarbeit by Tobias Hackel "Measurement of interface-deformation in a two-fluid-system influenced by mechanical oscillations" [Hackel] describes the use of a laser vibrometer to measure the interface shape.
The pneumatic shaker used for the experiment was constructed by Sascha Jung as another Projektarbeit [Jung]. Both the mechanical setup and the control via PC and TestPoint were designed by him. He also conducted first observations of fluid systems on this shaker.
The last Projektarbeit to be mentioned here was written by Olaf Baudisch and was finished in spring 2004. The focus was on the installation of a rotating copper-electrolyte system, forming the experimental basis for the Galinstan-electrolyte experiments.

1.4 Main steps of this work

Before the beginning of the work, magnetic field measurements had been made at a rotating system (solid copper and KOH) with a single sensor and several mechanical components of the present experiment existed (pneumatic).
At first, the behavior of the closed two-fluid system was investigated on an electromagnetic shaker and an excitation frequency was chosen. These parameters were then tested with the pneumatic shaker. A first multi-sensor configuration was set up. Mode detection and interface reconstruction were found to be possible. The interface movement and certain electrochemical properties of the system were documented. The usability of vibrometers to measure the interface deformation was tested. The amplitude of the interface movement was reduced by a new electrolyte and first test with a different mode were performed. An improved second multi-sensor configuration was prepared.

Chapter 2

The experimental setup

This chapter does not contain a complete description of the experiment but certain features and problems shall be described if they seemed important.

2.1 Pneumatics

The shaker is driven pneumatically, because unlike an electromagnetic shaker, it does not generate an elektromagnetic field. The control is rather simple, as no proportional valves are used, but simple on-off devices. Still, this showed not to be hindering the experiment. The amplitude of the vibration is controlled by a mechanical construction limiting the movement range of the cell. A pressure of 5 bar showed to be good to drive the experiment, higher pressures made the flatcable fall off from the sensor board.
The valves are switched by a black-box-device, which again is controlled by the Keithley card (an AD converter) in the measurement computer. A TestPoint-program allows to generate control signals with different frequencies.
The movement of the shaker and the cylinder is also very close to a rectangular signal, regarding vertical position as a function of time (figure 2.1). This was checked by an inductive probe.
The peaks following each drop seem not to be related to the behavior of the board or the cell, but to the probe itself, "bouncing" like a ball after hitting the ground (the number of bounces decreases if the shaker is operated with lower pressure). A similar phenomenon occurs if the probe has the possibility to move higher than the board. In this case it lifts off after upward acceleration.
The amplitude of the shaker was about 0.9 mm in this configuration. Higher amplitudes (1.12 mm) also work, but smaller amplitudes like 0.45 mm and 0.6 mm do not excite the desired mode.
From the measurements it can be found, that the shaker frequency is in fact the desired 7.25 Hz (figure 2.2, 2.1). This is found both in the time and frequency domain.

It should be pointed out, that for several measurements it was not the central pressurized air system, that was used, but a small laboratory compressor (Jun-Air 6-4).

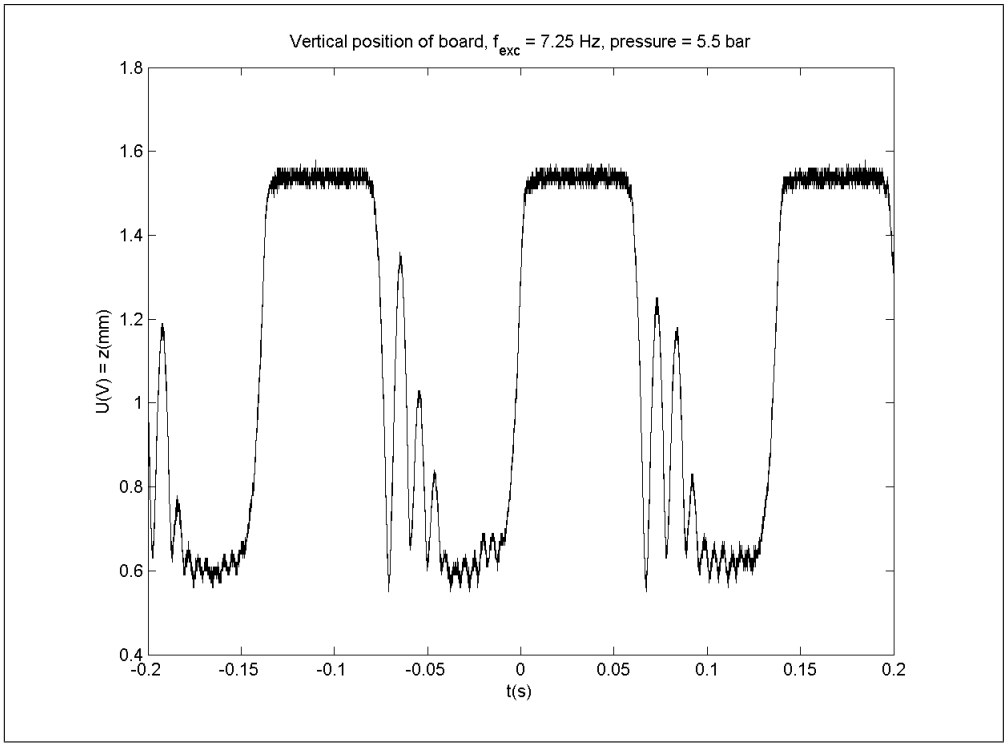

Figure 2.1: Vertical movement of pneumatic shaker, 7.25 Hz (exct.)

2.2 Geometry

The geometry of the experiment is needed both for the numerical modelling and in order to compare the measured and the calculated data. It is especially important to agree upon the definition of the vertical position (of the interface, the sensors, ...). Images of the existing experimental setup can be found in figure 1.1, a schematic plot of the future setup with rotatable sensor board is found in figure 2.3. Here you will find the cell in cyan-color, the base plate in light grey, above the additional plate in red and the sensor board in dark grey. Notice the openings in the red board allowing to change the position of the sticks holding the sensor board. Also notice, that the sticks (grey) are usually covered by husks (blue). They consist of several pieces of known length and ease the vertical positioning. This principle was already introduced for the existing setup.

- z=0 is at the upper side of the plate glued to the bottom of the cylinder. Attention: For the second sensor board, another plate is placed on top of this one
- The base copper electrode has got a height of 2 mm. It is found between z=0 mm and z=2 mm
- With current applied, the Galinstan surface is found at z=50 mm
- The screw fixing the bottom electrode from inside the Galinstan is approx. 3 mm high and about 7 mm in diameter.

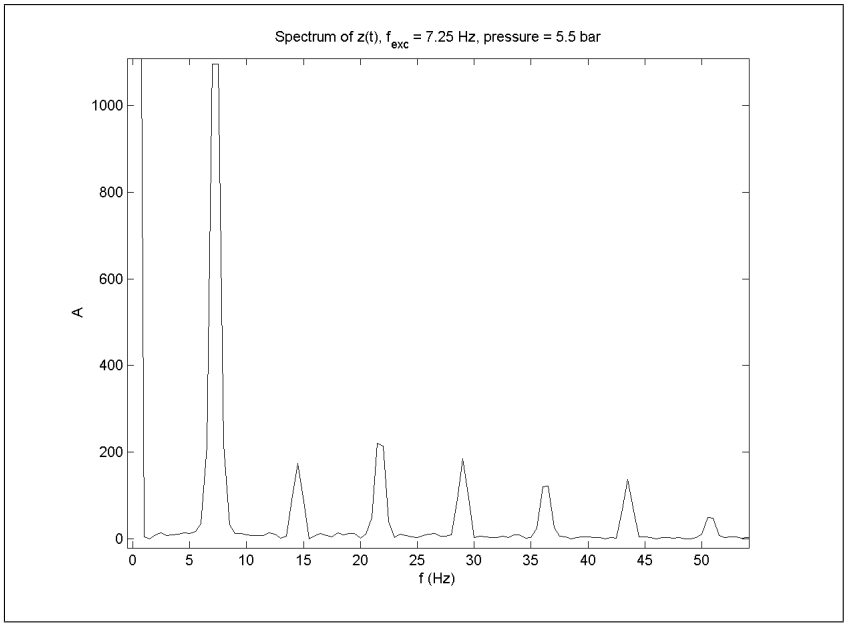

Figure 2.2: Spectrum of vertical movement of pneumatic shaker, 7.25 Hz (exct.), 24.06.04

- The position of the first board is given by measuring the height of its upper side
- The horizontal sensors' centers are 25 mm above the first board's top side and 10.25 to 12.25 mm away from the plexiglass wall.
- The vertical sensors' centers are also 25 mm above the board's tops side and 11 to 11.5 mm away from the plexiglass wall
- Both sensor types are 15 mm long and have a diameter of approximately 1.5 mm.
- In azimuthal direction, the vertical and horizontal sensor of one pair are separated by a plate of 1 mm thickness.
- The additional plate allowing to rotate the second sensor board is 8 mm thick.

2.3 Chemical

As a liquid metal, Galinstan is used. Galinstan is the eutectic alloy of

- Gallium 67%
- Indium 20.5%
- Tin (Sn) 12.5%

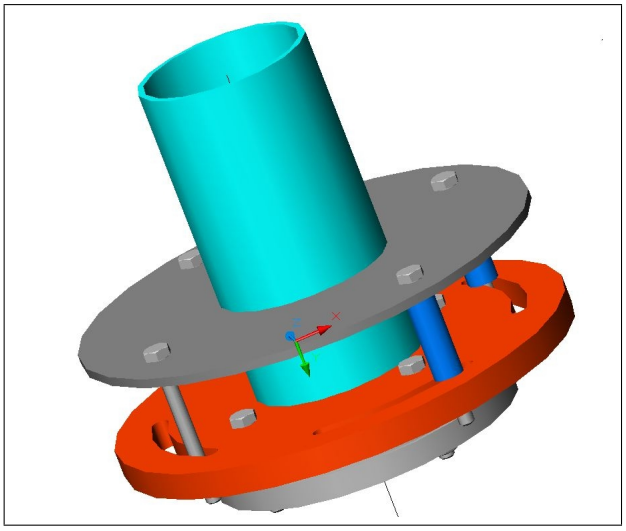

Figure 2.3: Sketch of the setup with rotatable sensor board (grey), based on additional plate (red) with long openings

and liquid at room temperature. It is quite similar to mercury, but not as dangerous.
As an electrolyte, an aqueous solution of potassium hydroxide (KOH) is used. It is a lye fluid.[1] The KOH solution is 2 molar, that means 2 mol of KOH are dissolved in 1 liter of water. That is equivalent to 112g KOH in 1 liter or 10 % (weight). The density of such a solution is 1087 kg/m^3 at 25 degree Celsius.

Previous configuration

In the previous experiments (copper-KOH), the polarity of the voltage driving the cell current was (+) up and (-) down. This configuration suffered from the fact, that during the experiment, electrolysis of water took place. At the Anode (+) O_2 was produced ($2H_2O \rightarrow O_2 + 4e + 4H^+$) and at the Cathode (-) (the copper surface) H_2 developed ($2H_2O + 2e \rightarrow H_2 + 2OH^-$). As a result, (optical) measurements were possible for a few seconds only, after the current had been switched on, because then the gas had formed bubbles that rose from the interface.

New configuration

The number of bubbles inside the electrolyte could be reduced by a suggestion of U. Schmidt from FG Elektrochemie. It is based upon the fact, that Galium dissolved anodically at the bottom electrode. Only the polarity of the experiment needed to be changed to (-) up and (+) down.
Still H_2 develops at the top but these bubbles do not pass through the main volume of the cell. At the bottom, Ga is anodically dissolved in small amounts, and forms more complex OH reaction products (black dirt). For our experiment, this is a good

[1] Within this and other documents, the electrolyte is sometimes referred to as "KOH". Of course it is an "aqueous solution of KOH".

configuration. First experiments are described in ([SieSch04]). Here interesting surface behavior of Galinstan (change of surface tension, movements) was observed. No photographs were taken at that time, but one can find detailed information and images in chapter 3. More important, in the later experiments, the amplitude of interface waves was significantly reduced when current was applied.
The loss of Ga during these experiments can be calculated using the Faraday law:

$$m = \frac{M}{F \cdot n} \cdot I \cdot t \tag{2.1}$$

Here, m is the electrochemically converted mass (g), M is the molar mass (g/mol)[2], n is the number of electrons per single reaction, F is the Faraday constant (96487 As/mol), I is the current (A) and t is time (s) [Heitz86].
One can say, that the loss of Galium during my work was acceptable small, as the Galinstan is still usable[3].
Additional experiments were performed using a solution of Fe^{3+}, sulphuric acid and water as electrolyte, but did not give the desired results, as the electrolyte was destroyed by chemical reactions with the Galinstan.
If the experiments is repeated several times a day, a silver-colored layer (Galium) builds up on the copper electrode.
In the previous experiments, the KOH solution was found to be corrosive towards copper parts immersed into it. These effect are not troublesome, if the top electrode is removed after experiments, washed and kept dry. The silver-colored layer can also be reduced, if one applies a current with inverse polarity for several minutes.
Anyways, the KOH solution should be replaced after experiments, to remove the reaction products from the system.
Another reaction is predicted at the contact interface between Galinstan and the copper base electrode. Copper will be dissolved by the Galinstan to form a new alloy. The timescale for this reaction is unknown. Nothing related to that phenomenon could be observed.

Current density distribution

The question has been brought up, whether the current density distribution in the cell is really homogenous. This was mainly triggered by the fact, that non-homogenous material transport is a main problem in electroplating and treated explicitly in the literature.
In our case, one can say, that the assumption of a homogenous distribution can be made, as long as the top electrode and the Galinstan surface cover the whole diameter of the cell. For example see [Wagner51].

Different amplitudes

It is desirable to be able to excite different amplitudes inside the cylinder. A dependence of the excitation amplitude or pressure was not observed. The mode simply

[2]Ga: 69.72g/mol

[3]The properties of Galinstan are based upon the fact that it is eutectic, so this is not as self-evident as one may think.

does not occur for small amplitudes and does not change for higher excitation amplitudes. A possible way to change the amplitude might be a change of the cell current. By changing the surface tension, the amplitude might change as well. The disadvantage of this method is, that the current also directly affects the signal intensity. So this method was not used.
Instead, it was tried to change the viscosity and it was found that the mode amplitude is reduced, if the viscosity of the top liquid is increased. For this purpose, glycerol was added to the KOH solution.
In order to "design" an appropriate solution of KOH, water and glycerol, one has to take the following facts into account:

- For any electrolyte, the conductivity will decrease, if the viscosity is increased (movement of the ions is hindered). One can say, that conductivity * viscosity = constant.

- The conductivity of solutions of KOH in water has got a maximum for a certain weight ratio (That is, one cannot increase it endlessly). Lower and higher amounts of dissolved KOH reduce the conductivity. For solutions of KOH and water, the maximum conductivity is found for 30% (weight) of KOH. [4] There is not data available for solutions of KOH, water and glycerol.

- For solutions of water and glycerol, the viscosity can change strongly. Compared to pure water, the viscosity of a 1:1 mixture has increased by approximately 5 times and rises exponentially for higher amounts of glycerol.

See appendix F for details. The new solution was designed to have a viscosity about 5 times higher than water and the highest possible conductivity.
The new solution consists of :

- 50g water (34.965 % weight)

- 50g glycerol (34.965 % weight)

- 43g KOH (30.07 % weight)

Attention: This mixture has to be treated with care. It has a **ph-value of 11** or above and is therefore **strongly erosive**. It also becomes hot during the mixing process. The color of the solution is slightly yellow. It seems not to be erosive to plexiglass.
It showed, that this mixture has got a too high viscosity and damps all interface motion for $f_{excit} = 7.25$ Hz and 5 to 3 bar shaker pressure. But if water or KOH solution are added to the cylinder (about 30 to 40 ml), modes are found. The conductivity is satisfying. The solution allows a cell current of 1 A at a voltage of about 5 V [5]. See 3.4.1 for more details.
The density of the solution is found between 1238 and 1336 kg/m^3. Compared to the density of pure glycerol (1265) and 30% (weight) aqueous KOH solution at 15

[4] By now, the ratio is about 11%. Even though the tabled data is limited, one can expect the conductivity to rise by approximately 50%

[5] Compared to about 2.2 V for ordinary KOH solution. But all these values depend on the properties of the interface as well.

degree Celsius (1300) [D'AnsLax49], this value seems quite reasonable.
Measurements were performed (**??**) in order to investigate the dependence of the interface amplitude on the used solution. It showed, that it can be changed from 8 (7) mm (if an electrolyte with glycerol is used) to about 12 mm (in the case of 2 molar KOH solution). One must notice, that for certain solutions, a wave motion appears only without current. The solution allowing minimum amplitude has not been completely determined. But a volume ratio of 7:3 (new solution mixed with 2 molar KOH solution) is still having a slightly too high viscosity. Therefore, one should try volume ratios of 6.5:3.5 or 6:4 (new electrolyte:2 molar solution).

2.4 Electrodes

Copper plates

The electrodes used for the experiment are both copper plates. The base plate is fixed by a screw inside the Galinstan. From below, at the bottom side of the cylinder, the screw is fixed with a plastic plate, a cable shoe and a screw-nut. The current is supplied from the side, i.e. in a non-axisymmetric way. This could not be avoided, because space is limited due to the shaker.
The top electrode has got a completely flat low side and four small openings at the side in order to let gas leave the fluid. A vertical stick is attached to it and allows a very symmetric current supply from the top.
The top and especially the "bubble escape paths" should be modified. For example, the black screw-ring holding the electrode from the top, does not touch the wall in the area above the electrode and below thread. In this space, bubbles are caught and re-injected into the fluid when the cylinder is shaken.

Glass Plates

As it was planned to combine magnetic and laser measurements, an electrode was designed to fulfill 3 tasks: To cover the fluid with a fixed wall (no slip condition), to serve as an electrode and to allow visual observation.
For this, a glass plate was chosen, that was coated with conducting paths. Previous plans to use completely coated plates had to be abandoned, as the conductivity was to low. The glass plates covered with ITO have a resistivity of 10...100 Ohm/Square [6]. Compared with the resistivity of the electrolyte ([Dobos75]), which is in the magnitude of 0.01 Ω/m, this is about two dimensions too high, the current will rather enter the electrolyte directly [7].
At first a circular glass plate was cut and a central hole drilled by a university craftsman, then the paths were imprinted by FG Mikroperipherik. The design of the paths was designed by me, the according AutoCAD file was generated by B. Schütze. See figure 2.4 for details.

[6] That means any square area with current injection on one and ejection on the other side will have this resistance. The thickness of the conducting layer is included in the given value, and length and width of the current path will compensate each other

[7] There are also plates with higher conductivities available from Taiwan, but the plate we have are from Saarbrücken with the values given above.

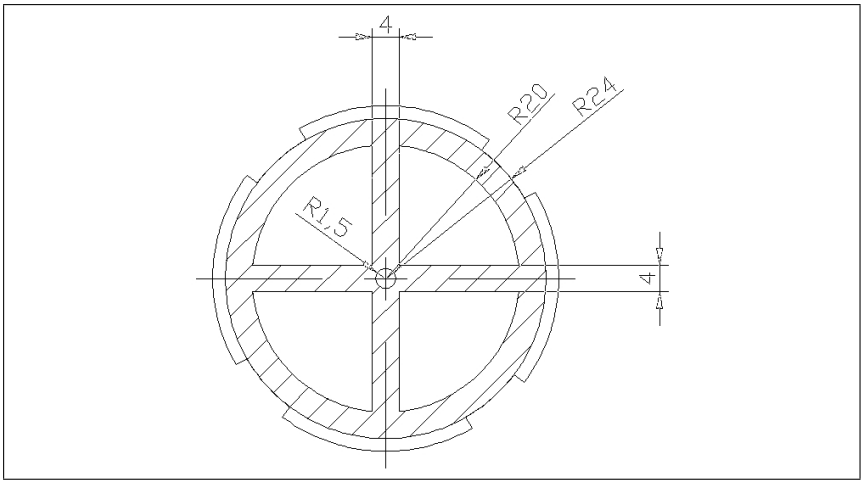

Figure 2.4: Top electrode design

It showed not to be possible to solder the printed conducting material. Still, by mere mechanical contact an electric contact was achieved as well. A first coating material based on "plastic" and silver was mechanically and chemically non-sufficient. A new electrode was made, based on silver and glass. In tests, this material was not destroyed, but showed signs of fatigue.
The glass plate did not go into practical use, because the vibrometer tests failed.

2.5 Sensors

The sensors used in the experiment are fluxgate sensors from Aviatronic Ltd. They provide a measurement range from 0 to 100 μT.
The experiment uses 8 sensor pairs equally distributed around the cylinder. A sensor pair measures the local vertical and radial component of the magnetic field.

2.5.1 Sensor qualities

As the fluxset sensors had not been used before, it was necessary to check their qualities.
The sensor was placed inside a pair of Helmholtz coils. The sensor was connected to an oscilloscope (HAMEG HM 1507-3 or Tectronix TDS 3034B) and current supplies for power and offset voltage. The magnetic field of the coils was controlled by a voltage source and tuneable resistors. The magnetic field strength was measured not only by the sensors, but also by a Gaussmeter (Wutronic).
The experiment did not aim at optimized measurement conditions, but at conditions similar to the board and to generally investigate the behavior of the sensors (offset, noise, signal).

For the sensor check, the flux density was varied between -40 mT and + 40 mT in the horizontal axis and was kept at earth field level in the vertical direction. The change of direction in the horizontal direction was possible, because the coil field

was oriented in the opposite direction as the natural magnetic field. The resolution of the Hall probe is 1 μT. But the measured field was varying within a range of about +/- 2 μT and exact conformity of the sensor's and the probe's axis was not assured.
For the horizontal sensor, the output voltage was measured for two fixed offsets (2.5 V and 3.5 V) while the flux density was changed and for the smallest possible flux density (200 Ohm resistance) the output voltage was measured depending on the offset.
For the vertical sensor, the output was measured depending on the offset (for weak horizontal field, 200 Ohm) and for 3 different flux densities in horizontal direction (high amplitude in 2 directions, weak amplitude) in order to get an idea of the direction sensitivity.

2.5.2 Results

The following main results were found:

- The dependence of the output on the flux density is linear
- The output voltage decreases linearly with increasing offset voltage, from 4 to 0 V
- The output voltage factor (voltage/flux density) is usually found to be in a range from -20 to -21 $\frac{mV}{\mu T}$. With regard to the limited exactitude of the method, this is no contradiction to the value given (18.5), but this problem should be kept in mind.
- Higher frequencies were found to be superimposed on the DC signal (figure 2.5).

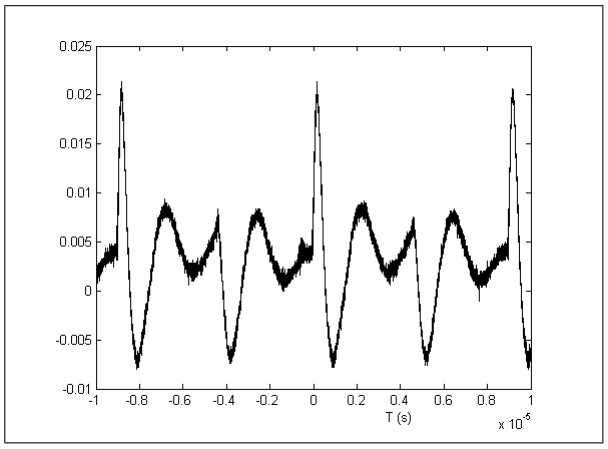

Figure 2.5: Interfering signal, the amplitude is unclear, as the 50 Ohm impedance of the oscilloscope was used

2.6 Hardware-Software-Interface

The signal path from the sensors to the PC's hard disc consists of six main parts:

1. Printed Circuit Board
2. Cables
3. A data collection board by Keithley
4. Cables by Keithley
5. AD converter on a card inside the PC by Keithley
6. TestPoint software

Of these, number 3 to 5 are fixed. The main point is to design 1 and 2 well and to connect this construction in a good way to 3. For the power supply of the sensors, additional features need to be included in 1 and 2.
Two designs were developed. The first one was used to for the measurements described in the following chapters. The second one is supposed to replace the first one in order to improve the signal quality. Both shall be described below.

2.6.1 Electrical setup

The first setup was based upon a common ground for all sensors, flat-cables, a PCB that could only be moved in the vertical direction, a power supply taken from the Keithley board and offset voltages derived from this voltage by two resistors. The measurement mode was "single-ended". A data collection program was developed.

First Printed Circuit Board

The sensors were mounted on a printed circuit board (PCB). The board met the following requirements:

- Vertical positioning of the sensors. This is achieved by sticks with thread that are fixed to the bottom plate of the cylinder. Cylindrical shucks around the sticks are used to define the height, the sensor board is placed on top and everything is fixed by screws from above.
- Voltage, offset voltage, signal transfer. The power voltage is distributed to all sensors from one origin, the ground is distributed by two paths.
- 4 holes for positioning the board by vertical sticks
- a separate offset line for each sensor
- 2 connection pads

The board was realized in cooperation with the PCB-laboratory of the Department of Mechanical Engineering.
Two flatcables are attached to the board. Their configuration is as follows: There are two pin groups with a flatcable each. The left one is located on the low side of the board, the other one on the top side. The one on the low side may fall off, if the pressure driving the shaker is higher than 6 bar. Starting from the left (the red cable in both cases) (in world coordinates when looking towards the board), the cables have the functions described below. The connections can be found in appendix C. The sensors are numbered starting at the sensor in the front, most close to the low contact line and being placed between two holes. Then, the index increases in clockwise direction.
The voltage supply showed unexpected properties. It delivered not the expected 5.00 V but 5.14 V (0.04 V can even be measured between +5V and Ground when the computer is switched of). The voltage also did not decrease as fast as it should have been expected (5V - 10 Ohm $\cdot$ n $\cdot$ 5 mA). For 7 sensors, the voltage still was 4.96 V.
Due to the design based on two connection pads only, the paths on the boards are rather long. Not only do they need a lot of space on the board (limiting the number of sensors), but they also make intense use of the top side, where they are exposed to chemical and mechanical stress (screw fixing).
Measurements by Dr. Men had suggested, that increasing the offset voltage would reduce the noise on the signals delivered by the sensors. Therefore, experiments with increased offset voltage were performed on at a later stage of the experiment. The offset voltage used here was 3.8 V. The originally intended voltage of 4 V could not be achieved. The sensors' inner resistance between the Offset and the Ground pin is rather low (about 8400 Ohm) and as the sensors are electrically parallel, the range of the voltage divider was limited.

2.6.2 Second Printed Circuit Board

A new PCB was developed during the work, but not jet used. It features

- AC lowpasses for all sensors in order to assure the sampling theorem
- a single shielded cable for each sub-sensor
- short paths on the board
- paths on the low side of the board
- improved mechanical fixing of the cables
- The board can be rotated. This is achieved by fixing the sticks on an additional plate with circular elongated holes. Here the positioning of the sticks is possible at any desired angle. The disadvantage of this approach is limited space to move the sensors. Positioning the sensors below the interface is not possible.
- data connection and power supply by separate board close to the Keithley board

The voltage and signal distribution will be eased by another PCB that will be positioned close to the Keithley contact board.

2.6.3 Some measurement modes

The AD converter on the Keithley card comes with several features, which are intended to increase measurement exactitude.

Uni/Bipolar

The working range of the AD converter can be changed from +/- 10V to 0..10 V. Use the AD object and the "Other AD command" with "unipolar" and "yes/no". This command is not documented in the standard documentation, but see [KeithleySupport04] or appendix D.

Gain

Before AD conversion, the signals can be analog amplified. TestPoint will than rescale the signals. This command should increase the resolution, but in single-ended mode, no effect was found.

Single-ended vs. differential

Single-ended: All sensors share one common ground, only one wire per sensor, 32 sensors possible, for strong signals only
Differential: Signal high and signal low for each sensor, 16 sensors possible, sensors should float, changes in the LinxDriver and the data collection board necessary, for weak signals

2.6.4 Trends

Measurements using more boards at one time are desirable. If a certain design of PCB has been found to be good, one might solder the sensors directly on the board instead of using mechanical fixings.
It is also planned to design boards which can carry more sensors (10, maybe 12).

Chapter 3

Optical measurements and observations

This chapter contains 4 main parts.
The first section (3.1) describes the results of a first mode investigation on an electromagnetic shaker. Even though several modes between 5 and 20 Hz were found, only one stable mode was to be chosen for the future experiments.
The second (3.2) is based on video measurements giving qualitative insight on the behavior of the interface under different conditions.
The third (3.3) gives the results of experiments with laser vibrometers.
The final part (sections 3.4.1, 3.4.2) deals with the test of a new electrolyte (section 2.3).

3.1 Top view observation of interface oscillation modes

For identifying stable modes and in order to get their characteristics in detail, the following experiment was performed:
The cylinder was filled with Galinstan up to a height of 50 mm, the rest of the cylinder was filled with HCl acid (approx. 2.5 %). The cylinder was then placed on an electromagnetic shaker. The experimental setup was covered with black cloth in order to shield it from direct light. A circular light source (neon lamp) and a mirror for the observation were placed above the cylinder. Without any deformation of the interface, two shining rings were observed at the contact of Galinstan and the wall. Deformation of the interface caused other areas to reflect light towards the mirror, forming characteristic patterns. The resolution of course is somewhat limited, as only stronger inclinations are seen. A high speed camera (VDS Vossmüller GmbH) was placed besides the experiment and the interface was observed via the mirror.
The cylinder was then exposed to forced vibrations of different amplitudes and frequencies ranging from 5 Hz to 20 Hz in steps of about 0.5 Hz. Image sequences were taken. These sequences were sampled with 21 images per second, allowing to check for frequencies up to 10 Hz [1].

[1] Actually the sampling rate was twice as high (42/s), but due to a camera bug, only every second image was exported.

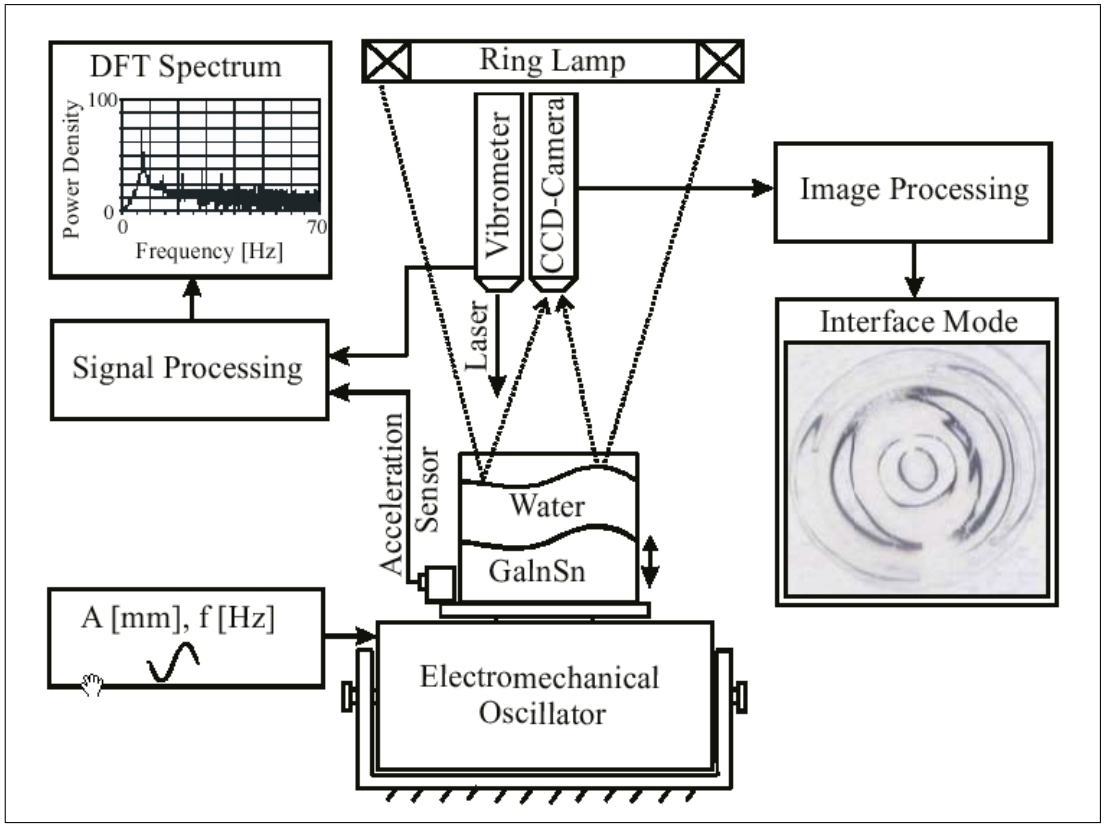

Figure 3.1: Sketch of ring light observation setup

Observation was slightly hindered by gas bubbles, that developed on the metal-electrolyte interface and that also rose to the glass cover. Removing the bubbles from the glass was only possible when the cylinder was kept in a non-horizontal position and the bubbles were loosened from the surface by small impulses, making them rise towards the holes. a schematic sketch can be found in figure 3.1.

The following results can be taken from the experiment:

- Several modes exist in the frequency range investigated during the experiment
- The mode type depends both on the frequency and the amplitude, modes different from circular rings usually appear for higher amplitudes
- Around 7.5 Hz, a non-radialsymmetric (1,1) mode could be observed (figure: 4.10).
- The amplitude of the (1,1) mode was several mm, therefore higher than expected
- It is not clear, whether the (1,1) mode was "pure" or affected by higher harmonic modes
- The optical measurements both from above and from the sides give good insight into the fluid movement

Frequency (Hz)	Effects
5.53	axisymmetric rings
5.79	moving "moons"
7.10	(1,1)-mode
7.52	(1,1)-mode
7.79	(1,1)-mode
8.49	chaotic
10.05	(2,1)-mode
11.55	chaotic
12.25	(3,1)-mode
14.77	(4,1)-mode
17.73	(5,1)-mode
19.53	(6,1)-mode

Table 3.1: Mode structures on electromagnetic shaker

In table (3.1), one can find the surface effect caused by stronger excitation. In case of small amplitudes, the resulting surface movement generally are axisymmetric rings.
There are also two figures of wave patterns, showing the (1,1)-mode (figure: 3.2) and a higher mode (figure: 3.3).
The (1,1) mode was chosen for further investigation, as it offered a unique amplitude and a simple structure, which is necessary as the limited number of sensors does not allow to reconstruct complex structures (sampling theorem in space).

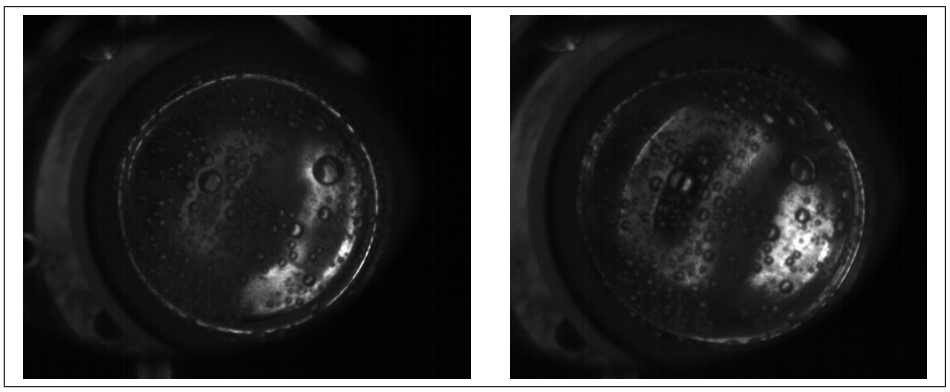

Figure 3.2: Galinstan surface shape at 7.52 Hz excitation frequency, illuminated by ring light and captured by high speed camera from above

Figure 3.4 shows a comparison of an image of the (2,1) mode that was made during the experiment and a plot of isolines of the interface based on a numerical calculation of the interface [Kuilekov]. Even though the basic features are similar and easy to compare, one can see that there are several structures superimposed in the experimental image.

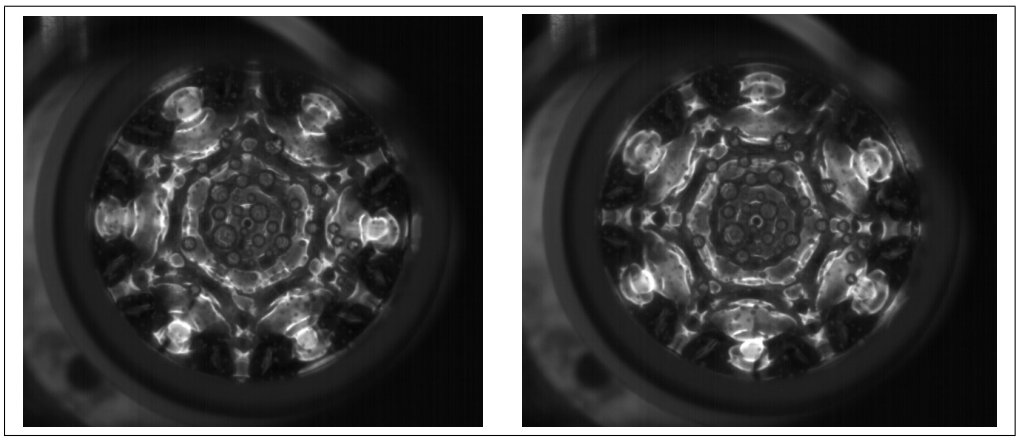

Figure 3.3: Galinstan surface shape at 19.53 Hz excitation frequency, illuminated by ring light and captured by high speed camera from above

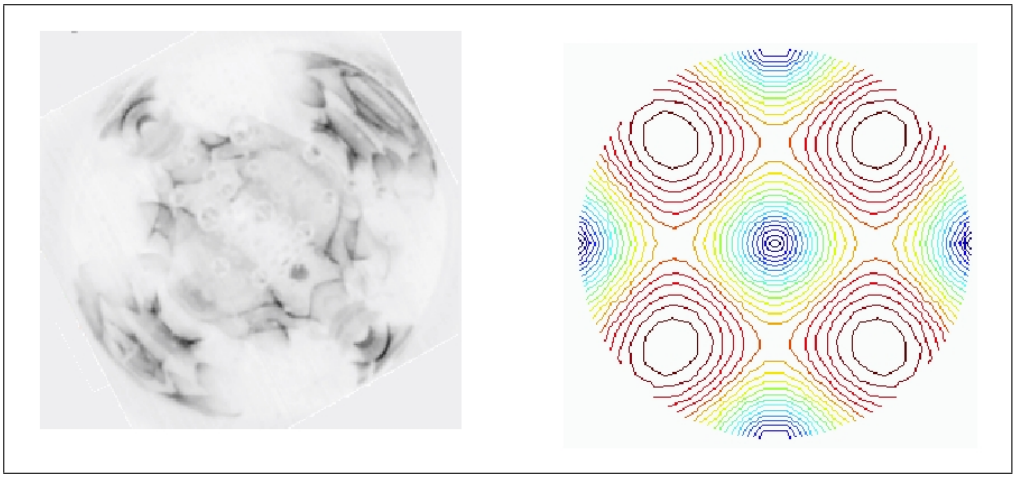

Figure 3.4: Comparison of (2,1)-mode image and calculated interface

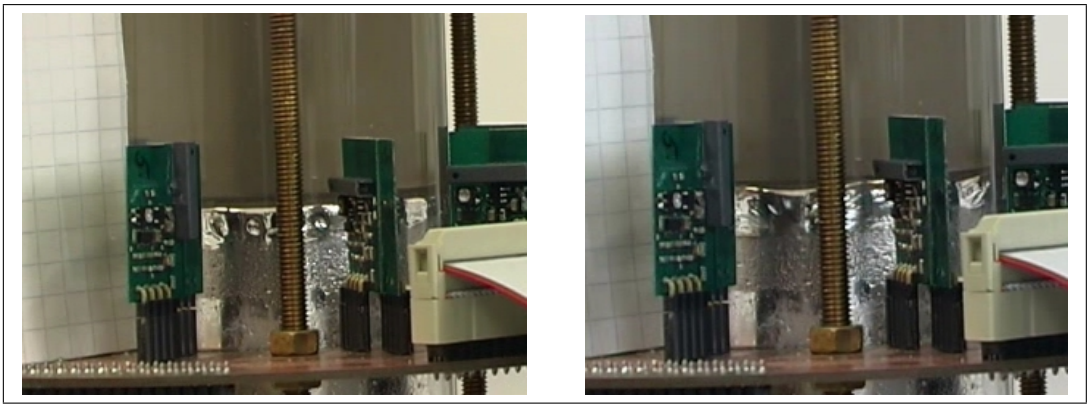

Figure 3.5: Interface effects due to cell current, 0.5 A vs 1.0 A, no shaker, notice the flat surface (no meniscus and the effects on the sides: different zones, ripples, movement

3.2 Side view video observation

For the video measurements a Canon XL 1s PAL camera was used. The camera can also serve as a video recorder and data can be exported to a computer via a FireWire-connection. The program used here is Pinnacle Studio. It allows to cut the video data and to save it as .mpg files.
The surface behavior was documented for different conditions (Cell current on/off, vibration on/off). The shaker frequency was 7.25 Hz (also 7.5 Hz for some video measurements, but this frequency was not used further).
From single images taken from the video material, one can estimate the amplitudes [2] . They are:

- 16 mm for 0.0 A
- 16 mm for 0.5 A
- 11 mm for 1.0 A

It can be observed, that large bubbles below the top electrode impede the build-up of the mode. So it seems like a closed top is necessary for the excitation of the mode.
As mentioned before, the top of the Galinstan becomes flat when current is applied and there are movements at the sides, that can be observed through the plexiglass (3.5). The phenomenon may be explained as electrocapilarity.
Notice the three different zones. The moving top zone has a shining surface, the middle zone has got a shaded surface with bubbles and the lowest region has got a shining surface again.
The interface deformation can become very strong for 0.5 A, generally stronger than for 1.0 A. For 1.0 A, "tension ripples" dominate, while for 0.5 A there is real movement.

In figure 3.6 one can find the interface deformation in case of an excitation with 7.25 Hz. The result is a strong wave with a broad peak.

[2]Visual observation on other days rather suggested values of about 8 mm for the damped wave at 1.0 A, but later measurements for the new electrolyte gave similar values.

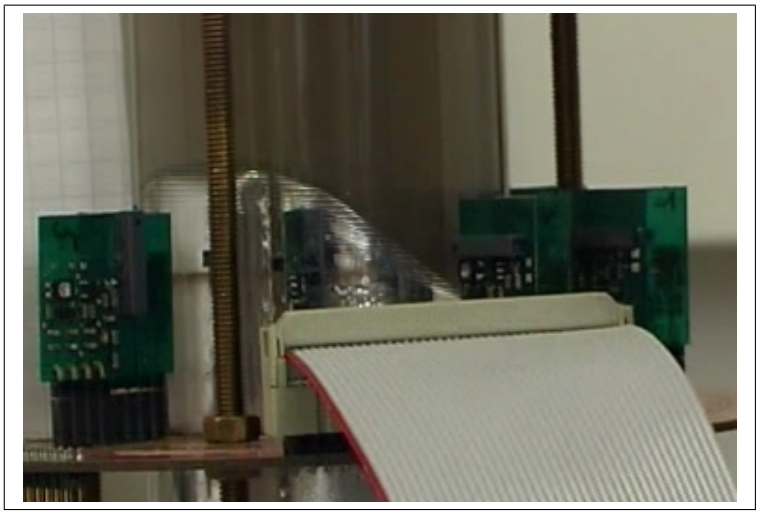

Figure 3.6: Interface oscillation, (1,1)-mode, maximum amplitude, 7.25 Hz excitation frequency, no cell current, wide peak and high amplitude

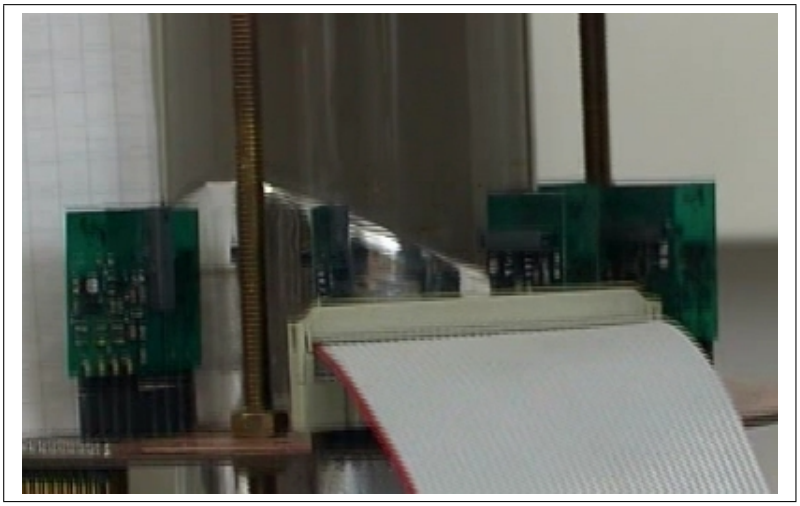

Figure 3.7: Interface oscillation, (1,1)-mode, maximum amplitude, 7.25 Hz excitation frequency, 0.5 A cell current, peak becomes narrow

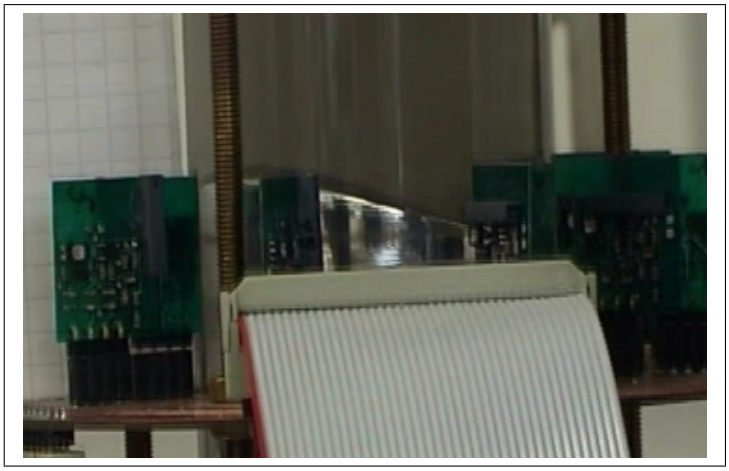

Figure 3.8: Interface oscillation, (1,1)-mode, maximum amplitude, 7.25 Hz excitation frequency, 1.0 A cell current, amplitude decreases compared to 0A

This shape is already changed if 0.5A is applied additionally. The peak decreases in height, but mainly becomes smaller (figure: 3.7).
For 1.0 A, the amplitude and the shape change once more (figure: 3.8). The amplitude decreases for about 5 mm compared to the amplitude without current. The shape is quite similar to the shape at 0 A. Looking at the surface and not the contact area of metal and cylinder, one can say that the shape is generally concave and not flat.

3.3 Laser-vibrometer

Two laser vibrometers were used:
The Portable Digital Vibrometer PDV 100 an the OFV 502 by Polytec. Both use visible red light. The raw signal is transferred to a measurement computer via a VIB-Z-012 Juction Box and a PC card. Data processing can be done using VibSoft 80 software, provided with the vibrometer.
The vibrometer velocity signal of the PDV 100 shows a DC-offset. According to the Polytec support this is in accordance with the device's specifications and suppressed in case the FFT representation of the data is used. In this case, the amplitudes for all frequencies shall be correct, i.e. the amplitude of a measured vibration is not affected by the constant DC part of the velocity signal.
The PDV is a very compact device with control unit and optics together, while the OFV 502 needs an external control unit (OFV 3000). Unlike the PDV, the laser beam of the OFV is not emitted directly, but via a flexible glass wire. Still, according to my experiments and the Polytec support, the small measurement head makes it sensitive to direct reflections only, while he PDV can more easily deal with diffuse reflected light.

3.3.1 PDV 100

Measurements using the PDV laser vibrometer and the (1,1)-mode without current flow were carried out. For that purpose, the top of the cylinder was covered with a glass plate. Three different setups were tried:

- Simple mirror above cylinder, vibrometer on a tripod
- Surface mirror above cylinder, vibrometer on an optical bench
- Vibromter above cylinder

Even though the test used different configurations it was not successful. The signal quality for nearly all measurements is bad or a signal does not exist at all. It is already very difficult to get a good signal quality (the vibrometer has an indicator for that) when the interface is at rest. Except 3 measurements, no data set showed amplitudes of more than 2 mm. About 5 mm were measured twice, one measurement gave even higher amplitudes. But this measurement could not be repeated.
There can be several reasons for this failure:

- There are several medias and their interfaces involved, air, liquid, glass, liquid, metal, so the beam will measure these interfaces as well or the beam will easily split
- Bubbles often form below the glass cover
- The interface has got strong inclinations when moving, reflecting the beam away from the vibrometer. It is also difficult to assure an exact orthogonal laser beam, as the positioning of the vibrometer or the mirror can be difficult.
- The maximum of the (1,1) mode cannot be observed, because parts of the interface are covered by the black top ring. This point might be helpful, as it has got a horizontal inclination even when the wave reaches its maximum.

The settings used were 500 for the velocity (0.125)[3], 22kHz cut-off frequency for the lowpass and no highpass. On the PC, the spectral representation was preferred, as it allowed to observe the appearance of a 3.6 Hz component directly, including its amplitude.
The single successful try (figure: 3.9)deserves some attention, as it shows very interesting features: The amplitude of the (1,1) mode is changing periodically over time. Of course there is no way to say if this is some measurement error caused by whatever properties of the system or a true result. Still, should this be a feature of the interface movement, future measurements will have to measure amplitude and magnetic field simultaneously ! It will not be possible to rely on the stability of the interface movement.
Figure 3.9 contains the amplitude in mm for 3.59 Hz extracted from the spectrum of each single measurement. The data is plotted according to the index of the measurements, the initial index number is randomly chosen. Each measurement lasted for about 6 seconds and approximately 4 seconds have to be added for saving the data and starting the next measurement. So the time difference between each measurement is approximately 10 seconds.

[3]Make sure, that the parameters are also set at the PC

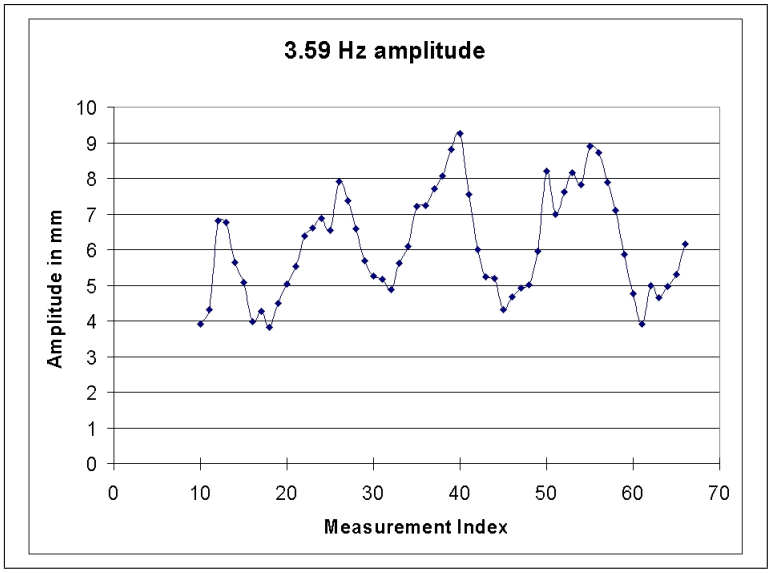

Figure 3.9: Amplitude of 3.59 Hz component of interface movement for several successive measurements with laser vibrometer, 1 measurement is approx. 10 seconds

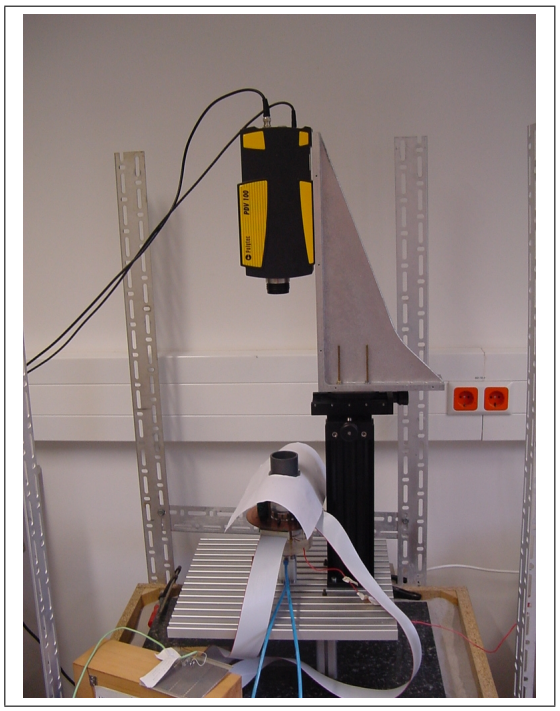

Figure 3.10: Measurement setup used for laser vibrometer, the paper sheet is used to protect the sensors from ejected electrolyte

3.3.2 OFV 502

The test of the OFV 502 failed even more than the previous measurements. The OFV may be a mighty tool, but it is also very demanding concerning the measurement environment. If it does not receive a strong direct reflection, it fails to generate a signal. The PDV 100 is easier to use. One simple example: If an ordinary sheet of white paper is placed in the beam of the PDV and the beam is focused on the sheet, a good signal quality is achieved. The OFV hardly reacts, even when focused.
The measurement setup was very much the same as before. The OPV 3000 control unit was placed on a table beside the experiment, together with a PC. Additional to the previous measurements, it was also tried to reduce the influence of the reflected light by black paper around the experiment instead of white paper (the paper is shielding the room from random laser beams) and to cover the experiment by a transparent layer in order to catch some of the reflected light indirectly. As the OFV is very unsensitive to anything except direct reflection, this failed. Finally it should be mentioned that the lens of the vibrometer is very sensitive and easily de-focused by the weak vibrations of its positioning device.

3.3.3 Possible improvements

For future measurements, the Polytec support recommended to position the laser vibrometer as close to the cell as possible (even below the optimum working range), in order to capture as much light as possible and to make strong use of lowpasses (both at the vibrometer and in the software). For the first point, it was recommended to shield the vibrometer by a glass plate positioned non-orthogonal to the beam. This way, reflections should not influence the vibrometer, as they do not reach it.

3.4 Variation of Amplitude

3.4.1 New KOH solution

In order to "fine-tune" the numerical algorithms it is desirable, to get magnetic data for one mode but different amplitudes. The new solution of KOH, glycerol and water which was made for this purpose (section: 2.3) was tested on 10.08.04 in order to analyze the resulting amplitudes and effects related to it. The test was documented using the video camera known from previous measurements.
For the camera measurements, it was tried to keep the camera on the height of the fluid interface. Length scales were attached to the sticks usually holding the sensor board.
Measurements were made for the ordinary 2 molar KOH solution, the pure new solution and several mixtures of the new solution with water and KOH solution, as its viscosity was too high and damped all movement. The measurements were started with the pure new solution and the given amounts of water/KOH-solution were used to replace a part of the previous electrolyte. So each new line in the following table starting from line "25ml water" is a modification of the previous

solution, not a completely new one.

Solution	Ampl. for 1A (mm)	Ampl. for 1A (mm)	U for 1A (V)
2 molar	13.75	12.5	-
new	0	0	4.8
25ml water	6.25	0	-
10 ml KOH	8.75	7.5	2.8
2*10ml KOH	10	8.5	1.8
5ml KOH	11.5	8.75	-
2*5ml KOH	11.25	10	-

3.4.2 8 mm Amplitude

Based on the test described above, optical and magnetic measurements were performed for a glycerol-water-KOH solution. A first attempt using a volume ratio of 7 parts new solution and 3 parts 2 molar solution failed, because when cell current was present, the interface movement was suppressed. Again, 10 ml of solution inside the cell were replaced by 2 molar KOH-solution.
This solution led to an amplitude of 8 mm with cell current, and 9 mm without cell current. The electrolyte was used for one day and became very dirty. Even though, measurements taken in the morning and evening showed no difference in the amplitudes, so the mechanical and electrical properties of the electrolyte seem to stay stable.
The amplitude of 8 mm is nearly identical to those amplitudes derived from visual observation. Still, taking the first camera measurements and the test of different solutions into account, one has to accept, that visual observation easily fails, while the results of the camera measurement can be reproduced. So even for the older magnetic measurements without camera check, one should assume about 12 mm instead of 8 mm.
But one should also notice, that the difference between current and non-current measurements has become smaller with regard to the first camera measurements. This might be a measurement error, but I rather tend to believe that this is a first sign of the property change of the Galinstan used in our experiments.

3.5 Conclusions

Optical measurements are an integral part of the experiment, but did not proceed as much as desired. Even though it showed that optical information can easily be gained from the sides by a camera. This method is very powerful, but suffered from the fact, that the data evaluation took several days each time and was of limited exactitude. With the introduction of a CCD camera, this time scale might be reduced enormously and it may become much easier to clearly detect the interface amplitude peaks. Optical measurements for every magnetic measurement (instead of visual guesses) will increase the reliability. This is especially important with regard to unknown parameters such as ageing Galinstan.
Concerning the additional introduction of a laser lightsheet, one should be aware of the fact, that the sensor ring(s) will hinder optical access, when magnetic data is

gathered. One should separate the exact determination of the interface shape (laser lightsheet) and magnetic measurements. Still, the CCD camera (without lightsheet) should always be used for the determination of amplitude.
The laser vibrometers did not deliver the expected results. This does not mean, that they may not be used for certain tasks (frequency measurements, measurements of small amplitudes), but they are no "all-purpose" tools.
The ring-light method may be used to gain qualitative insight into the interface behavior, but quantitative results should not be expected soon, especially as long as copper electrodes are used for the top electrode.

Chapter 4

Magnetic measurements

The electric setup used for the measurements described here is explained in 2.6. Information on the connections of the flat cables and the according pads on the Keithley board are given in appendix C.
One can divide this chapter into three main parts. At first, the behavior of the sensors on the board was investigated (section: 4.1). Then, AC measurements were performed. Different parameters and positions of the board were tried (section: 4.2). Finally, a first measurement using a new electrolyte resulting in a different interface amplitude and a measurement using the (2,1)-mode were carried out (subsection: 4.2.3, 4.2.4).

4.1 Sensor Check on Board

Measurements were made to analyze the behavior of the sensors on the board. It showed, that the sensors are working and very sensitive but that the environment is rather difficult. Some properties of the system and the signals:

- The software allows to shake and measure at the same time and the software allows to collect data from the different channels in any desired order.

- The DC components of the signal should not be regarded, as the are not reproducable. The values differ, when single sensors are taken of from the board or when only single sensors are used. Especially the values for the vertical sensors did not seem to represent the physical reality. For the horizontal sensors, the maximum difference between the different measured values should have been about 1.6 V ($20\frac{mV}{\mu T} \cdot (40\mu T - (-40\mu T))$ but was only found to be about 0.6 V. One can find examples of the results in 4.1, 4.2 and 4.3.
  Possible reasons are limited stability of the electrical configuration (voltage of power circuit, EMC) and metal parts in the vicinity of the experiment (cable duct on the wall).

- A frequency spectrum can be calculated, showing different spectra for horizontal and vertical sensors. In both cases, the DC part of the signal (about 1.9 V for the vertical and 2.8 V for the horizontal sensors) is about 1000 times stronger than the AC components. The horizontal sensor showed a peak at 50 Hz, very much energy around 170 and 250 Hz and another peak at 410 Hz

(see: 4.4). The vertical sensor showed a peak at 50 Hz and increasing energy from 250 Hz on, which did not exceed the 50 Hz peak (sensor 7 vertical) (see: 4.5). The frequency range below 20 Hz seems to be less affected by noise.

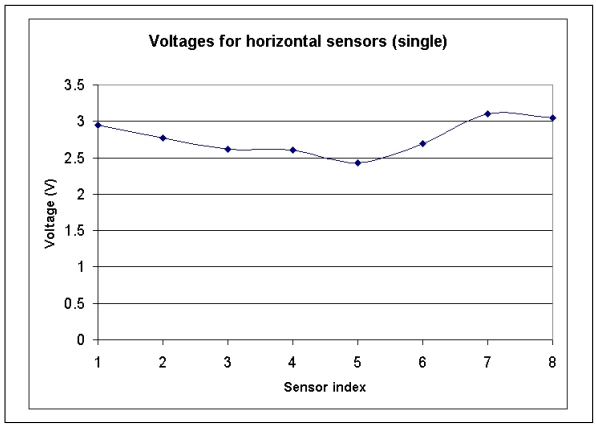

Figure 4.1: Horizontal voltages of the 8 sensors without cell current (only one sensor on the board each time)

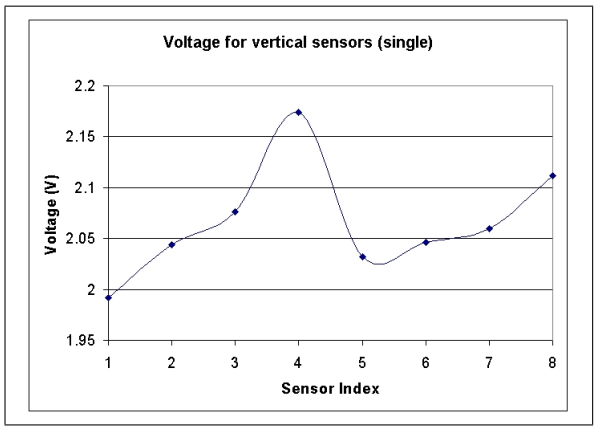

Figure 4.2: Vertical voltages of the 8 sensors without cell current (only one sensor on the board each time)

4.2 Interface measurements

4.2.1 Interface vicinity measurements

The measurement parameters were 5 s of time and 1024 S/s and the cell parameters I = 1 A and f_{excit}=7.25 Hz. The data was then shared with Fachgebiet Theoretische Elektrotechnik (FG TET). Here the data was processed for interface reconstruction as part of the B-2 project. This was generally done for all measurements. The cell current of 1 A was chosen, because a current of 0.5 A had shown to be too weak to

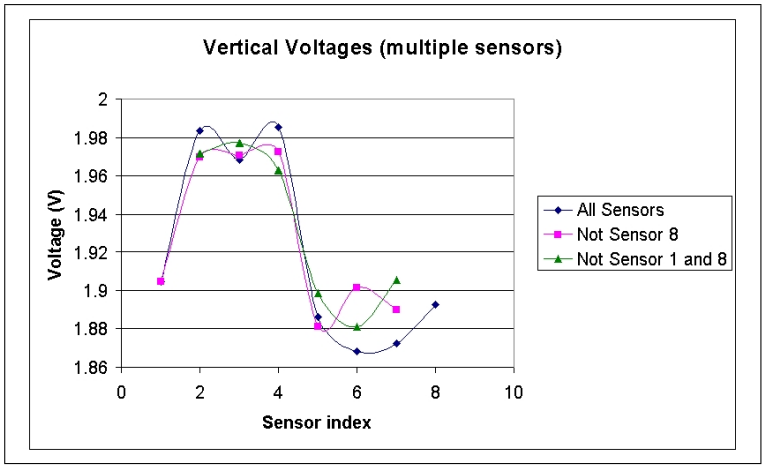

Figure 4.3: Vertical voltage measured with several sensors operating at one time, 02/03.06.04

generate signals detectable by FFT.
The cell current of 1 A was used in all future experiments.

In these measurements, the sensors were positioned near the interface, that is, the board was positioned at z=2.6 cm which is equal to the horizontal sensors at 5.2 cm and the center of the vertical sensors at 5.05 cm. FFT was used for first data analyzis.
The appearance of a frequency component at about 3.6 Hz can be seen both in figure 4.6 and 4.7. Of those, the later is more important, as it can be seen, that the peak is not caused by a single channel, but that most radial channels show the peak as a common quality.
The peaks were not found in the data of the vertically oriented sensors. This is because in the vicinity of the interface, no vertical component exists.

4.2.2 Variation of vertical position of sensor ring

The sensor board was placed at different z-positions and the magnetic field was measured several times with 5120 Samples/s for 10 seconds. These measurements were performed for offset values of 2.5 and 3.8 V. It showed, that an offset of 3.8 V tends to reduce the noise superimposed on the signals. Higher offset values shall generally be used in the future.
Measurement using the gain feature of the Keithley AD converter (that means, the signal is analog amplified before AD conversion) and the unipolar mode did not improve the signal quality.
The data showed the expected qualities. For example, as predicted by the numerical calculation, a vertical component of the flux density showed, when the sensors were positioned above or below the interface. It also showed, that the vertical component is generally weaker than the radial component (the maximum value is about half the maximum value for the vertical component) and therefore easier affected by noise. Examples of measured values can be found in figure 4.8 and may be compared to the calculated values for an amplitude of 7 mm in figure 4.9 (both taken from

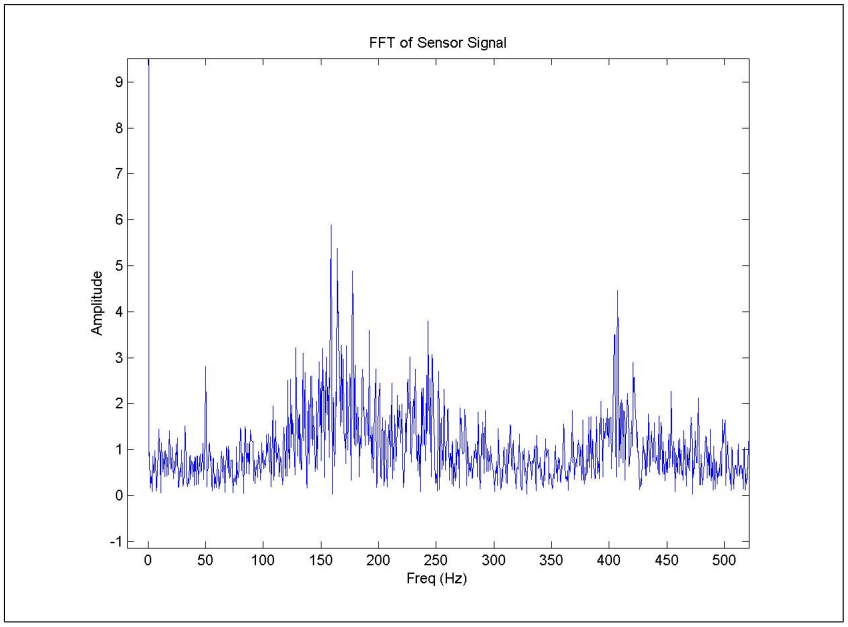

Figure 4.4: Detail of horizontal spectrum of single sensor, no cell current

[Ziolkowski]). A larger plot of the measured radial component can also be found in the appendix.

4.2.3 Variation of interface amplitude

In order to better calibrate the algorithms, it is desirable to measure the flux distribution not only for one interface shape and amplitude, but to change both parameters. The change of amplitude can be achieved by a new electrolyte with higher viscosity. This electrolyte allows to reduce the amplitude from about 12 mm (ordinary KOH-solution) to 8 mm. Of course, other amplitudes between those values are possible too. For a first measurement, 8 mm amplitude was chosen. The measurement conditions were:

- 10 seconds
- 5120 samples/s
- 3.8 V offset
- 8 mm interface amplitude

Mode detection and interface reconstruction was possible with this data, but detailed information is not jet available.

4.2.4 Variation of mode

Additional to the (1,1) mode that had been used for all experiments in this work, the (2,1) and the (1,2) mode were investigated. This measurement had two aims: Firstly, a mathematical model for the interface could be confirmed and secondly the

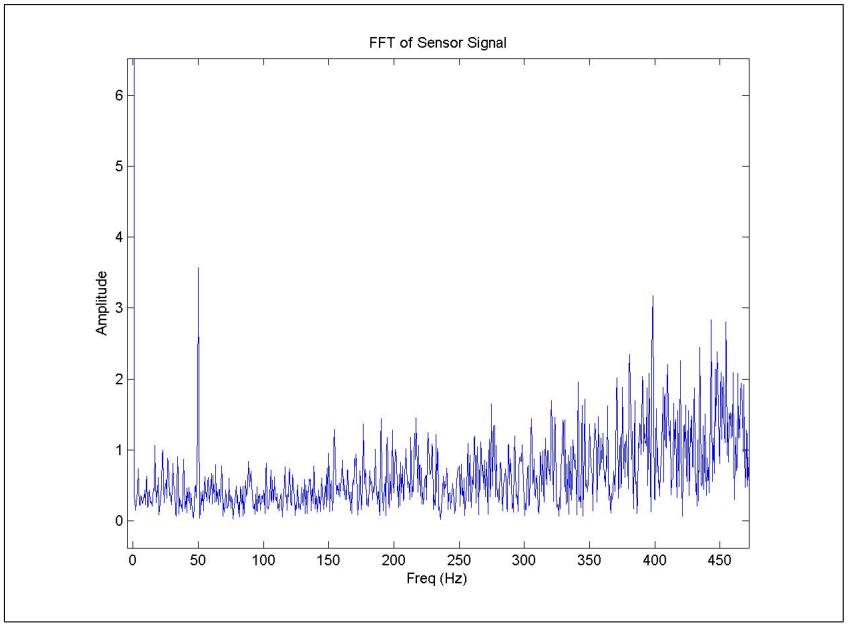

Figure 4.5: Detail of vertical spectrum of single sensor, no cell current

usability of other modes for magnetic measurements could be evaluated.
The first part of the experiment was very successful. Both modes were excited using a shaker frequency of twice the predicted interface frequency (just like for the (1,1)-mode) and in both cases, the predicted modes were found. Still it must be pointed out, that the interface frequency itself was not measured optically. It should also be pointed out, that the behavior of the modes with regard to the cell current differs: While the (1,1)-mode is easier to excite without cell current, both the (1,2) and the (2,1) mode could only be found when cell current was applied. Otherwise, strong random movement of the interface was found. This movement was suppressed by the cell current. Also see table 3.1.
The second part was partly successful. While the (1,2)-mode was rather unstable and did not generate a detectable magnetic signal, the (2,1)-mode was strong and stable and could be detected as a peak in the magnetic spectrum by means of FFT. The peak appeared at the predicted interface frequency of 4.7 Hz. For this measurement, only one z-position (chosen by FG TET) slightly above the interface was used.
The following table shows the parameters of the test:

Mode	predicted interface freq.	shaker freq.	results
(1,2)	6.21	12.44	exists, unstable, no magnetic measurement possible
(2,1)	4.7	9.4	exists, stable, peak in FFT of magnetic signal at 4.7 HZ

Figure 4.10 shows the shape of the (1,1) and the (2,1) mode and additionally the calculated radial flux component. The reduction of the expectable signal strength can easily be seen.

Figure 4.11 shows the peak of the (2,1)-mode at 4.7 Hz for 1 sensor. Figure 4.12

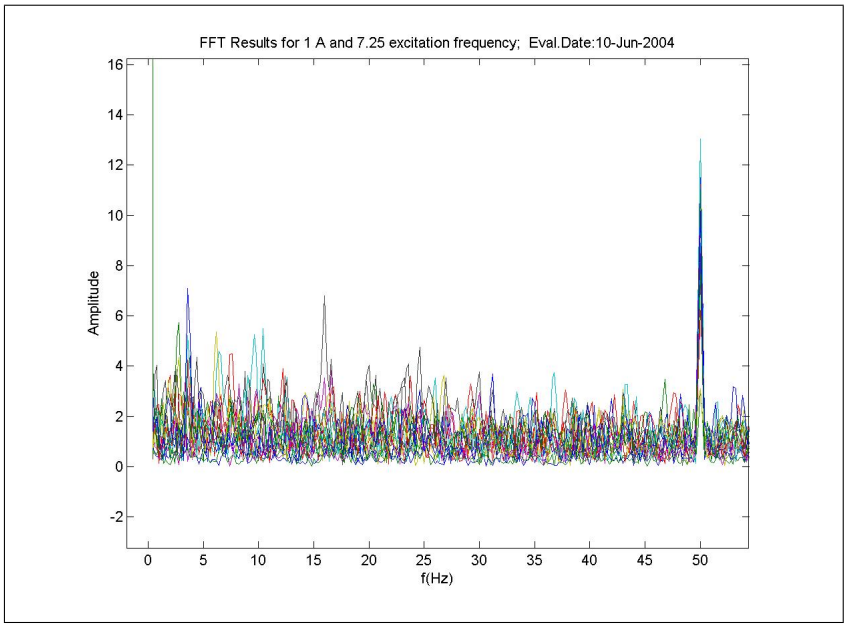

Figure 4.6: Spectrum of magnetic signal of all sensors for (1,1) mode, 7.25 Hz (exct.), 1.0 A, notice the strong 50 Hz peak and several single strong peaks

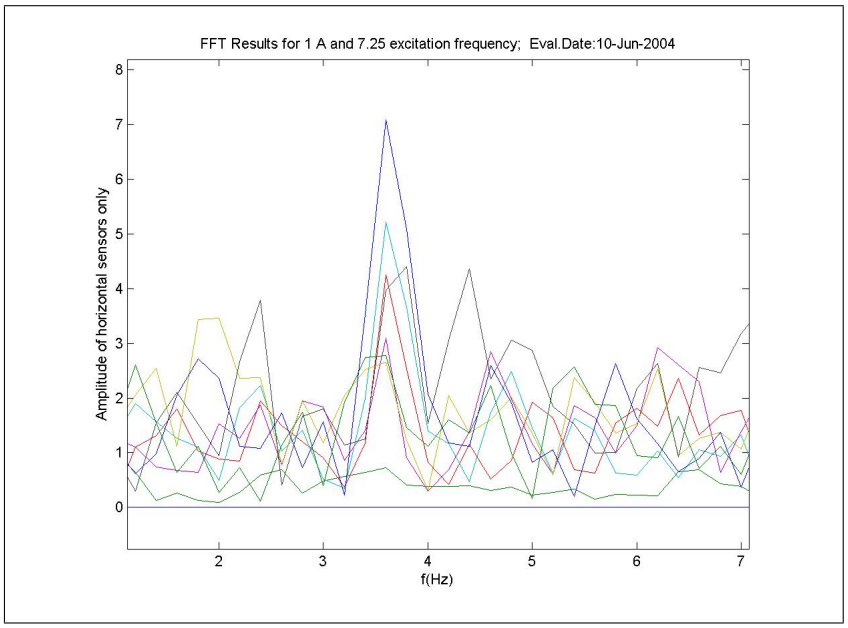

Figure 4.7: Spectrum of magnetic signal of radial sensors for (1,1)-mode, 7.25 Hz (exct.), 1.0 A, notice that this peak at 3.6 Hz is a common property of all channels, sensor position close to interface, no vertical signal here

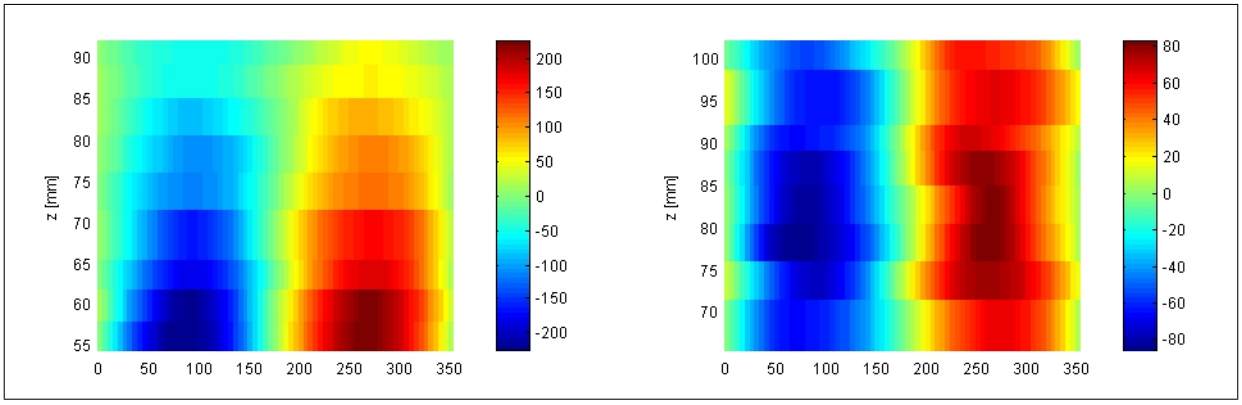

Figure 4.8: Measured flux density distribution for (1,1) mode, KOH-solution, 12 mm amplitude (?), x: angle, y: z-pos, color: flux, attention: covered measurement areas not equal

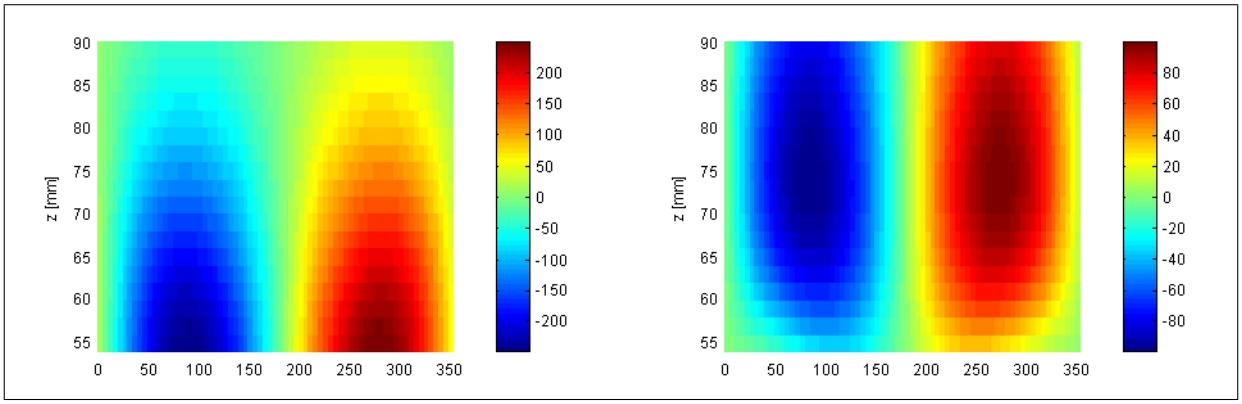

Figure 4.9: Calculated flux density distribution for (1,1) mode, KOH-solution, 7 mm amplitude, x: angle, y: z-pos, color: flux

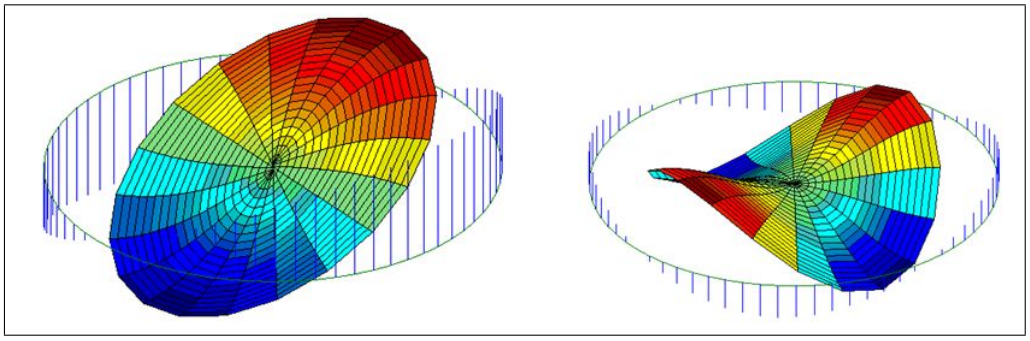

Figure 4.10: Calculated interface shape and radial flux component for (1,1) and (2,1) mode

shows the results for all sensors. It can easily be seen, that the more complicated structure of the mode and the flux density distribution as well as the smaller signal amplitude (about 50 nT compared to nearly 200 nT for the (1,1)-mode) do no longer allow to detect the signal easily by all sensors. Finally, figure 4.13 shows a comparison of the measured and the calculated flux density. But it should be pointed out, that for this experiment no exact interface amplitude data was gained, so the absolute values (not the shape) may differ for more exact measurements (All images taken from [Kuilekov]).

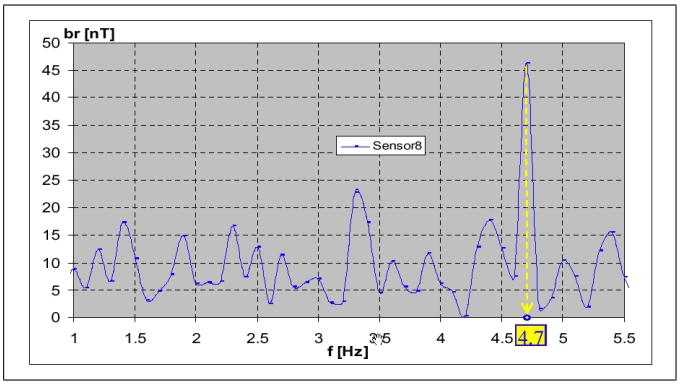

Figure 4.11: Magnetic flux density signal for (2,1)-mode for a single sensor

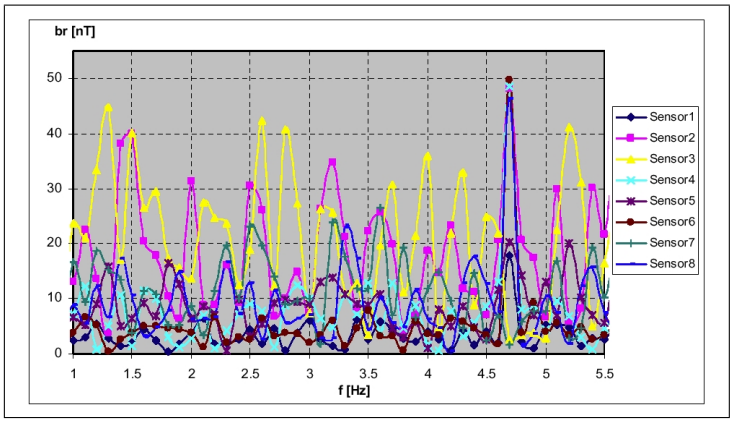

Figure 4.12: Magnetic flux density signal for (2,1)-mode for eight sensors

4.3 Conclusion

The magnetic measurements were very successful. The first multi-sensor configuration was set up and used. Interface reconstruction showed to be possible for strong amplitudes of the (1,1) mode and also for smaller amplitudes of this mode and the (2,1) mode. Generally, theoretical expectations and measured data are in good agreement, as a good measurement position for the (2,1) mode was chosen

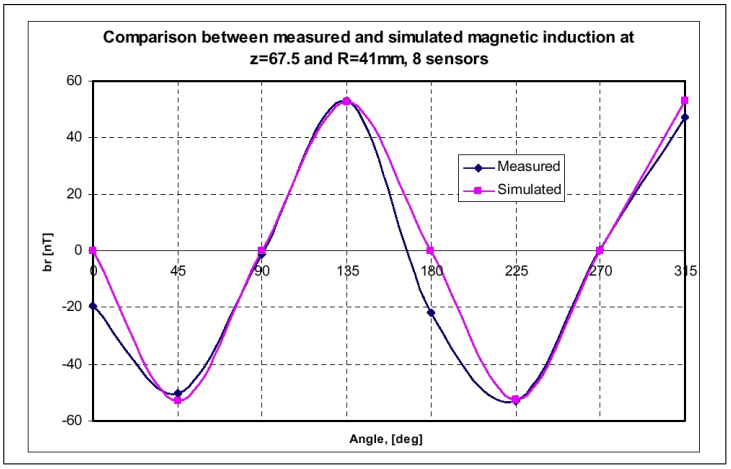

Figure 4.13: Measured and calculated flux density for (2,1)-mode

according to previous calculation of the field. Still it must be pointed out, that the magnetic data suffers from strong noise (especially for the vertical component) and many measurements cannot be used at all (more than 50%). In order to improve this situation advanced electrical set-ups have been prepared. These will hopefully help to improve the signal quality in general and reduce the number of measurements needed to get a data set of completely satisfying quality. It is also hoped, that a working mode of the Keithley card based upon (pseudo)differential connections will help to make better use of features like unipolar or gain.

Chapter 5

Conclusions

An experiment for magnetic and optical measurements of a fluid-fluid interface has been set up. It allowed to generate different interface modes and measurements using a magnetic multi-sensor system and different optical methods (camera, laser vibrometers). The flux density data gathered during the experiments makes detection and reconstruction of the (1,1) and the (2,1) interface mode possible. Additional experiments have been performed with a reduced amplitude of the (1,1)-mode. This was made possible by a modified electrolyte. An improved sensor setup has been prepared.
Please also refer to the conclusions at the ends of the previous chapters.

Appendix A

Addresses

- Polytec Vertriebs- und Beratungsbüro Berlin 6392-5140
- Vertrieb- und Kundenberatung Polytec 49(0)7243604178
- Leiterplattenlabor MB R.-D. Böhme, Tel.: 3873
  Laborgebäude MB
  Zimmer 1117
- Sigma-Aldrich, Chemicals
  www.sigmaaldrich.com
- Farnell, Electronic Components
  www.farnellinone.de
- Conrad, Electronic Components
  www.conrad.de
- Keithley
  www.keithley.com
  Roland Blumberg: rblumber@keithley.com
  TestPoint hotline: testpoint@keithley.com Tel.: 01805/534845
- Chemikalien:
  Frau Keller
  FG Elektrochemie und Galvanotechnik
  Werkstoffgebäude
  1. Stock, links, zweite Tür links

Appendix B

Documentation of TestPoint program

During my thesis, Mr Schütze worked in our group as a HiWi. His task was TestPoint programming and technical drawings. The following text is his documentation of the program he wrote in TestPoint. For the sake of simplicity it is not kept separately, but integrated into this thesis.

B.1 Vorweg

Dies "Programm" wurde im Rahmen der Diplomarbeit von Carsten Sievert zum Thema "Grenzflächenprojektion im TFD-Projekt B1 an der TU-Ilmenau" mit dem Programm "Testpoint" der Firma "Capital Equipment Corp" (www.cec488.com) erstellt.
Zur Datenaufnahme dient ein Hardwareboard der Firma Keithley (www.keithley.com), hierbei handelt es sich um das Modell KPCI-3116.

B.2 Überblick

Um Messungen durchzuführen, sollte es genügen,

1.) ein "lookuptable" über den Button `"lookuptable"`zu laden
1.b) Das Programm Shaker.tst auszuführen, falls die Messung an einem schwingenden Systems ausgeführt werden soll.(Parallel zu sievert.tst)
2.) die Parameter richtig anzugeben
3.) Die Werte mit "Übernehmen" zu bestätigen
4.) über "Messwerte aufnehmen" die Messung zu starten
5.) im sich öffnenden Dialogfenster einen geigneten Namen zu wählen (z.b. data00xy.DAT); hier werden ascii-dateien angelegt.
6.) Falls gewünscht, über den Button "FFT" die Signalverarbeitung zu starten.

shaker.tst

Dieses Testpoint-Programm sollte sich im selben Ordner befinden wie das "sievert.tst" und kann bzw. muss (falls es benötigt wird) parallel zum eigentlichen Programm laufen. Es ist als Modul aus einer älteren Arbeit übernommen worden und erwartet als Parameter die Eingabe der Frequenz, mit der der Zylinder angesteuert werden soll. Die Standardeinstellung liegt bei 7.5 Hz. Die Ansteuerung der Hydraulikzylinder erfolgt dann über ein Rechtecksignal. Der Schalter ist in der Standardeinstellung auf "on" gesetzt. Ansonsten sollte die Oberfläche selbsterklärend sein.

lookuptable

Der Button "opentable" lädt eine lookup-Tabelle, aus der Dateinamen fuer die einzelnen Kanäle bzw. Sensoren ausgelesen werden. Dies ist nötig, um die Werte der Kanäle in einzelne Dateien zu speichern und für diese Dateien Namen festzulegen.

Es wird zweispaltige (getrennt durch Tabulator) Datei erwartet, die in der zweiten Spalte die Dateinahmen in Anführungszeichen enthält. Ein Beispiel:
"0" "`s4_v`"
"0" "`s3_v`"
"0" "`s4_h`"
(...)

In einem Dialogfenster kann man die Tabelle auswählen. Derzeit enthält die Datei "lookup01" die Dateinamen.
Veränderungen dieser Datei können per Editor oder über das Programm "editlookup.tst" vorgenommen werden.
Die Länge der Dateinamen muss beibehalten werden, da es bei einigen Windows Versionen Probleme gibt, wenn Dateinamen mehr als acht Zeichen lang sind.
Im Programm nimmt das "Grid lookuptable" diese Tabelle auf und dient als Variable in späteren Funktionen.

Parameter

Die Parameter werden zusammen mit einem möglichen Kommentar in den Dateien abgespeichert.

Parameterliste
Folgende Paramter können gesetzt werden: (Die Werte in Klammern geben die default-Werte und die Namen im "Quellcode" an)

- "sample-rate" (1024, `P_sample_rate`)
  Sinnvoll sind Werte zur zweiten Potenz, da Testpoint dies für die Weiterverarbeitung (FFT) erwartet und diese sonst nicht fehlerfrei durchführt.

- Messdauer (2)
  `sample_rate` *Messdauer = Samples

- channels (03,02,01,00,23,22,21,20,04,05,06,07,16,17,18,19)
  Die Angabe eines Kanals ist unbedingt zweistellig anzugeben, weil dieser Paramter

als String eingelesen wird und die Position darin über `i*3+2` bestimmt wird.(i ist ein Schleifenindex von 0 bis zur Anzahl der eingegeben Kanäle-1). Die Anzahl der Kanäle wird bestimt, indem die Dimension der Matrix berechnet wird, die die Messdaten aller Kanäle aufnimmt. (grid "`alle_werte_matrix`")

Die Reihenfolge, in der die Kanäle eingegeben werden legt auch die Reihenfolge fest, wie die Kanäle in der Matrix abgelegt werden.

- "draw-channel-nr" (0)
  legt fest, welcher Kanal dargestellt werden soll. Die Nummer bezieht sich allerdings auf die Nummer in der "`Alle_Werte_Matrix`".

- "Messung-nr" (1)
  Hierbei handelt es sich um einen Zähler, der beim Start initialisiert. Es ist darauf zu achten dass die Zahl nicht grösser als 99 wird. "`messung_nr`" ist Teil des Dateinamens, welcher andernfalls länger als acht Zeichen werden kann und dann unter Umständen nicht mehr abgespeichert wird.

- "comment" ()
  Ermöglicht die Eingabe eines Kommentars, der, zusammen mit den anderen Parametern, in die erste Zeile der abzuspeichernden (Ascii-) Datei eingefügt wird.

- "Kanäle trennen"
  Auf "nein" gestellt beschleunigt dies die Messwertaufnahme, wenn man nur an der Matrix aller Werte interessiert ist. Dies übergeht die Schleife des Auftrennens der Matrix und des Abspeicherns der einzelnen Kanäle in einzelne Dateien.

- "gain" Diese Option erlaubt die Nutzung des Boardeigenen Verstärkers.

- "mode" Um Die Auflösung bei der Messung zu erhöhen, lässt sich hier der Modus von bipolar auf unipolar umstellen. D.h. Die Auflsung wird verdoppelt.

  Die Voreinstellung können ueber die Settings des jeweiligen Objektes geändert werden.
  Folgende Parameter werden den Dateien (in dieser Reihenfolge) in der ersten Zeile zugefuegt:

  - `sample_rate`
  - Messdauer
  - samples
  - date
  - Kanäle
  - comment
  - Gain

Das automatisches Hinzufügen der Parameter in der 1. Zeile einer jeden Datei kann wie folgt geändert werden: a.) komplettes Entfernen des Objekts der 10. Zeile in der action list "Messwerte-aufnehmen". (dann aber auch evntl. zugehörige Variablen entfernen: action list : "`parameter_list`" , Zeie 13-19 entfernen usw.) b.) durch Änderungen in der action-list übernehmen: hier "`set_cell_in`" variieren.

- **Zähler** Beim Start wird der Zähler über das Testpoint-feature des (nicht sichtbaren) Buttons "Zähler" initialisiert (Settings: "execute at initialize") und mit jeder weiteren Messung, die mit einem Klick auf "übernehmen" eingeleitet wird um 1 erhöht.

Übernehmen

Sind alle interessierenden Werte eingegeben, werden mit einem Mausklick auf diesen Knopf die Werte initialisiert, der Zähler erhöht und der Indikator gibt grünes Licht. Dies heisst jedoch nicht, dass alles sinnvoll eingestellt wurde !

Messwerte aufnehmen

Über ein "A/D-Objekt" wird auf das Keithley-board zugegriffen und die interessierenden Daten entsprechend den gewählten Parametern aufgenommen.

Die Rohdaten werden Testpoint-intern als Binärdatei unter dem den Namen "00xy.data.bin" abgespeichert, wobei "xy" mit jeder neuen Messung um 1 erhöht wird, sofern Dateien gleichen Namensschemas im selben Ordner vorhanden sind.

Die Rohdaten werden einer Variablen Namens "`alle_Werte_Matrix`" uebergeben, welche u.a zum Abspeichern als Ascii-datei dient.
Es öffnet sich ein Dialogfenster, mit welchem ein Name fuer diese Datei gewählt werden kann.
Sinnvoll wäre z.B 00xxdata.textbfdat.

In einer Schleife wird diese Matrix aufgetrennt ("sep-awm") und in die einzelnen Kanäle zerlegt, und abgespeichert (lookuptable).

FFT

Muss im Anschluss an die Messwertaufnahme erfolgen, da auf den selben Datenarray zugegriffen wird.
Es wird also immer die zuletzt erfolgte Messung verarbeitet. Die Namensgebung erfolgt analog zu der "`sep_a_w_m_subarray`", d.h. es wird auf den selben Datenarray zugegriffen. (vgl. "messwerte aufnehmen"). Die Darstellung der FFT verläuft unter Umständen nicht korrekt: Bei der Umrechnung der Amplitude und Phase vom Bogenmass in die Eulrsche Form "verwirft" Testpoint wichtige Daten, d.h. es werden von den Werten Zahlen abgeschnitten. Abhilfe schafft die Einstellung des Graphen in den Settings auf X vs Y"". Die FFT ist dann schwach als schwarzer Graph zu erkennen.

Dateien-ansehen

Es öffnet sich ein weiteres Panel, auf dem sich Dateien in Tabellenform und grafisch betrachten lassen

Dateien-bearbeiten

Es öffnet sich ein weiteres Panel, auf dem sich Dateien mit verschiedenen Fensterfunktionen bearbeiten lassen.

B.3 Zielstellung und Anforderungen

Anforderungen an das Progamm waren wie folgt festgelegt:

- **Parameterwahl:**

  Folgende Parameter sollten frei wählbar und nach möglichkeit mit einem sinnvollem Wert initialisiert werden.

  - Abtastrate(sample rate [1/sec])
  - Messdauer (time [sec])
  - Auswahl der Kanäle, bzw. der Sensoren, aus welchen Daten aufgenommen werden sollen
  - Anzahl der Stützstellen

- **Messung auslösen** Die Messung wird ausgelöst, alle ausgewählten Kanäle eingelesen und in einem flüchtigen Speicher abgelegt. Einzelne repräsentative Werte werden dargestellt (z.B. die Signale von 2 Sensoren als Plot über der Zeit), nicht zu viele, Übersichtlichkeit beibehalten.

- **Speichern der Daten in geeigneter Form**
  Die Rohdaten sollten unverändert gespeichert werden. Bezüglich der Form ist zu klären, ob es möglich und sinnvoll ist, ein file anzulegen oder mehrere einzelne (für jeden Sensor eine Datei), die in einem Ordner zusammengefasst werden. Vermutlich letzteres. Der Ordner muss einen Namen erhalten, der Nutzer muss Einfluss auf Ort und Name des Ordners haben, gegebenenfalls muss intern ein counter laufen, der dafür sorgt, dass unterschiedliche Messungen automatisch einen neuen Ordner generieren.
  Die einzelnen Dateinamen müssen einen Bezug zum Sensor haben, dessen Daten sie enthalten. Die unter Parameterdef. vorhandenen Werte werden z.B. als ASCII Datei automatisch mit in dem Ordner gespeichert, der die Messdaten enthält. Gut wäre auch automatisches Einfügen von Datum und Uhrzeit.

- **Signalverarbeitung**
  Für eine erste Beurteilung der Messergebnisse sind verschieden Formen der Signalverarbeitung anzuwenden. Z.B.:

  - Window (z.B. Hanning)

  - Fast Fourier Transformation (FFT)
    und oder
  - Filter
  - Window
  - FFT
    Die Anzhl der Samples muss berechnet oder aus der Parameterliste gewonnen werden.
  - grafische Darstellung representativer Werte

- **abspeichern der verarbeiteten Daten, unter einem eindeutigen Namen**

B.4 Sonstiges

B.4.1 Grafik

Die folgende Grafik soll das Prinzip des Programms veranschaulichen:

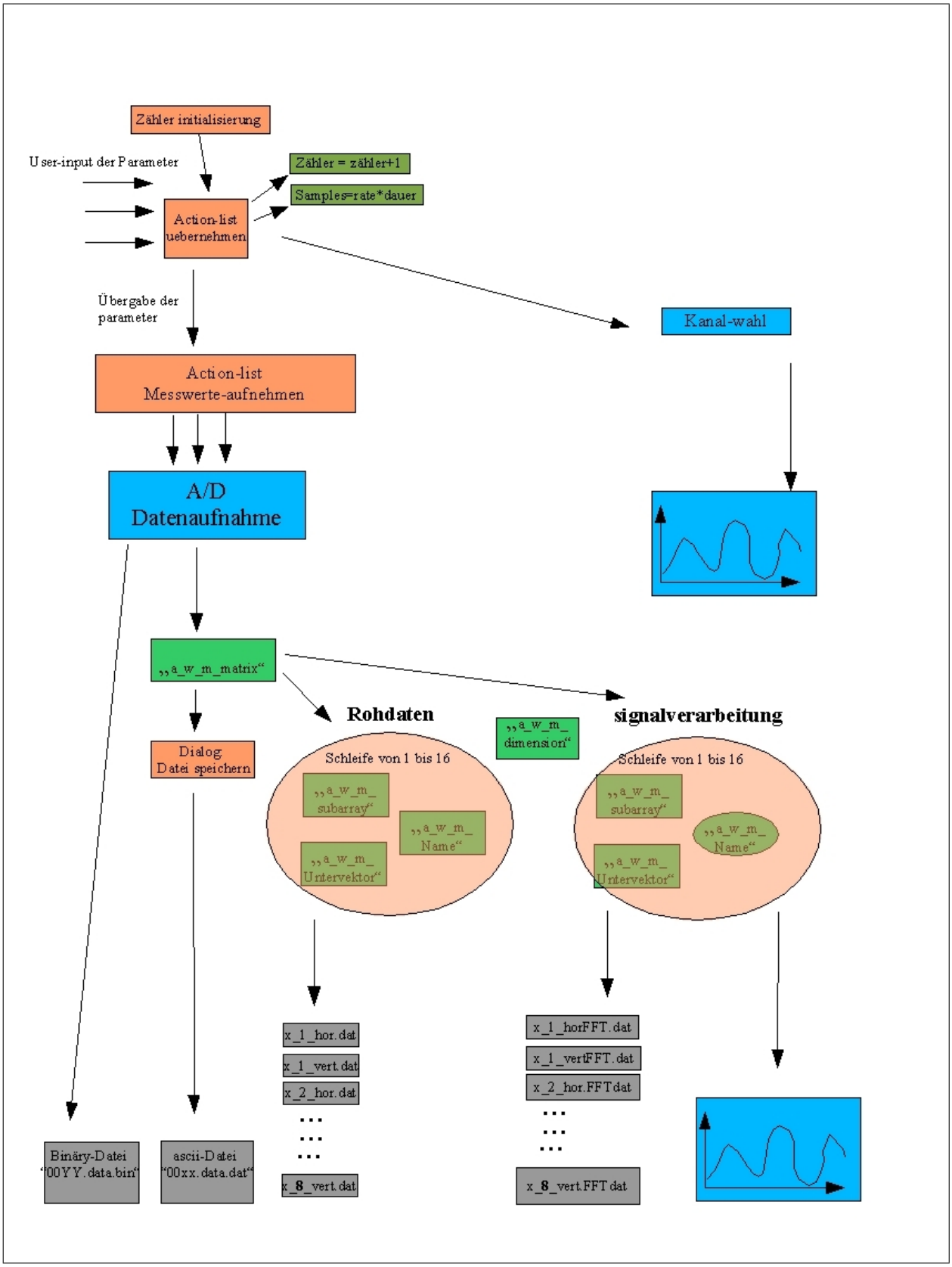

Figure B.1: Struktogramm

Appendix C

Wiring of first board

TB 34 (Analog Ground) and TB 38 (Power Ground) are shortcut with a piece of wire, to assure the voltage levels are identical.
In table C.2, VD is voltage divider, the supply of the offset voltage . It is a small circuit consisting of a fixed resistor (470 Ohm, later: 100 Ohm) and a changeable resistor (0..2000 Ohm). The voltage divider is connected to TB 112 (+5V) and TB 38 (Power Ground) on the board. The offset voltage is taken over the changeable 2000 V resistor. The voltage is distributed to all cables by a self-constructed board.
Therefore, two TB points have three connections going in:
TB 112: two power connections, voltage divider high
TB 38 : analog ground, board ground, voltage divider ground

Left pad

No.	Description	Pad	Channel
1	Sensor 4, vertical, Signal	TB 1	A In 0/0
2	Board Common Ground		
3	Sensor 3, vertical, Signal	TB 3	A in 1/1
4	Board Common Ground		
5	Sensor 2, vertical, Signal	TB 5	A in 2/2
6	Board Common Ground		
7	Sensor 1, vertical, Signal	TB 7	A in 3/3
8	Board Common Ground		
9	Ground	TB 38 (34)	Power Ground (Analog)
10	Board Common Ground		
11	5V (1, 2, 3, 4)	TB 112	+5V
12	Board Common Ground		
13	(not used)		
14	Board Common Ground		
15	(not used)		
16	Board Common Ground		
17	Sensor 1, horizontal, Signal	TB 9	A in 4/4
18	Board Common Ground		
19	Sensor 2, horizontal, Signal	TB 11	A in 5/5
20	Board Common Ground		
21	Sensor 3, horizontal, Signal	TB 13	A in 6/6
22	Board Common Ground		
23	Sensor 4, horizontal, Signal	TB 15	A in 7/7
24	Board Common Ground		
25	Sensor 5, horizontal, Signal	TB 17	A in 16/8
26	Board Common Ground		
27	Sensor 6, horizontal, Signal	TB 19	A in 17/9
28	Board Common Ground		
29	Sensor 7, horizontal, Signal	TB 21	A in 18/10
30	Board Common Ground		
31	Sensor 8, horizontal, Signal	TB 23	A in 19/11
32	Board Common Ground		
33	Sensor 8, vertical, Signal	TB 25	A in 20/12
34	Board Common Ground		
35	Sensor 7, vertical, Signal	TB 27	A in 21/13
36	Board Common Ground		
37	Sensor 6, vertical, Signal	TB 29	A in 22/14
38	Board Common Ground		
39	Sensor 5, vertical, Signal	TB 31	A in 23/15
40	Board Common Ground		

Table C.1: Board wiring 1

Right pad

No.	Description	Pad	Channel
1	Board Common Ground		
2	Board Common Ground		
3	Board Common Ground		
4	Sensor 3, h, Offset	VD	
5	Board Common Ground		
6	Sensor 3, v, Offset	VD	
7	Board Common Ground		
8	Sensor 2, h, Offset	VD	
9	Board Common Ground		
10	Sensor 2, v, Offset	VD	
11	Board Common Ground		
12	Sensor 1, h, Offset	VD	
13	Board Common Ground		
14	Sensor 1, v, Offset	VD	
15	Board Common Ground		
16	Sensor 8, h, Offset	VD	
17	Board Common Ground		
18	Sensor 8, v, Offset	VD	
19	Board Common Ground		
20	(not used)		
21	Board Common Ground		
22	5V (5, 6, 7, 8)	TB 112	
23	Board Common Ground		
24	Sensor 7, h, Offset	VD	
25	Board Common Ground		
26	Sensor 7, v, Offset	VD	
27	Board Common Ground		
28	Sensor 6, h, Offset	VD	
29	Board Common Ground		
30	Sensor 6, v, Offset	VD	
31	Board Common Ground		
32	Sensor 5, h, Offset	VD	
33	Board Common Ground		
34	Sensor 5, v, Offset	VD	
35	Board Common Ground		
36	Sensor 4, h, Offset	VD	
37	Board Common Ground		
38	Sensor 4, v, Offset	VD	
39	Board Common Ground		
40	(not used)		

Table C.2: Board wiring 2

Appendix D

Other AD commands

This chapter of the appendix is a mere reproduction of a Word-document by Keithley-Deutschland, giving some information on the Testpoint "Other AD commands" command. Of these, the last one is especially interesting, as it allows to reduce the range of the AD converter, a feature that is documented by Keithley for its hardware, but not by CEC for its software.

Additional A/D commands available on Keithley/Metrabyte boards
The following "Other A/D commands" are available on our Keithley/Metrabyte boards.

To use this commands, there is a difference between using the old "ASO" and the new "DriverLINX" driver.

You could use DriverLINX on Win95/98 and WinNT. If you don't have the 32 bit DriverLINX driver (DAS-8 series and DAS-1200/1400/1600 series), you should use the ASO driver, that means that you have to configure your board by running "CFGxxxx.EXE" file (xxxx stands for the board, e.g. 1600). Note: The ASO driver and the 16 bit DriverLINX driver will not work in WinNT.

To set an additional A/D command, you have to use the "Other A/D command" action. You can either use the pull down menu or write the command into the text field. The value is dependent of the driver you are using.

The additional A/D commands which are available are listed in the following sections:

1. Pre-Trigger
Description: Some A/D boards support "pre-triggering", which allows you to capture input data before the hardware trigger event.

Command	ASO (value)	DriverLINX (value)
pretrigger	e.g. 20	e.g. 20

Comments: (the value should be the number of samples you want before the trigger). The DAS1800 series boards (and above) support pre-triggering, with digital triggers. The DAS-50 and -58 boards support pre-trigger with either digital or

analog triggers. To disable pre-trigger, just set the of pre-trigger samples back to zero.

2. Simultaneous sample-and-hold

Description: If you have an external SSH option connected to your A/D board, you can sample multiple channels simultaneously (rather than at the A/D converter's conversion rate).

Command	ASO (value)	DriverLINX (value)
ssh	e.g. 1	

3. Burst mode timing

Description: In burst mode, you can set the time between channels, in units of usec (ASO) or ticks (DriverLINX).

Command	ASO (value)	DriverLINX (value)
burstticks	e.g. 20	e.g. 30

Comments: Note that burst mode channel/channel timing is in units of clock ticks in DriverLINX, which are 200nsec on the 1800 series. The burstticks command for Keithley boards in Win 3.x and Win95 (ASO) uses units of usec.

4. Synchronous A/D and D/A

Description: The DAS1800-AO and the KPCI-3108 boards have a mode where the same clock signal is used for both output (D/A) and input (A/D), so they are synchronized.

Command	ASO (value)	DriverLINX (value)
sync	e.g. 1	e.g. 1

Comments: - Give this command first, then start D/A, and finally start A/D. - This command sets the DriverLINX clock period value to zero for the D/A start command, which means to use the A/D clock. Note that support for this capability depends on the DriverLINX implementation.

5. Digital trigger polarity

Description: The default polarity for an external digital trigger (when enabled), is positive-edge. To change the polarity to negative-edge, use the following command.

Edge	Command	AS0 (value)	DriverLINX (value)
positive	ditrig	0	"+"
negative	ditrig	2	"-"

6. A/D Clock gating

Description: To enable an external gate for the A/D conversion clock, use this command:

Gate	Command	AS0 (value)	DriverLINX (value)
positive	gate	"+"	"on"
negative	gate	"-"	
no gate	gate	""	

Comments: Note that gate polarity is not setable in DriverLINX.

7. D/A Clock gating

Description: To enable an external gate for the D/A conversion clock, use this com-

mand:

Gate	Command	AS0 (value)	DriverLINX (value)
positive	gate	"+"	"on"
negative	gate	"-"	
no gate	gate	""	

Comments: Note that gate polarity is not setable in DriverLINX.

8. D/A digital external triggering

Description: To enable a digital start trigger event for D/A waveforms:

Value	Command	AS0 (value)	DriverLINX (value)
true	datrig	1	not supported
false	datrig	0	not supported

9. D/A gain (1800AO and KPCI-3108 models only)

Description: Set the D/A output gain. A gain of 1 gives a +/-5V range, a gain of 2 gives a +/-10V range on e.g. the 1800AO model.

Command	ASO (value)	DriverLINX (value)
dagain	not supported	e.g. 2

10. External clock polarity

Edge	Command	AS0 (value)	DriverLINX (value)
positive	extclock	not supported	"+"
negative	extclock	not supported	"-"

11. Bipolar/unipolar mode

Mode	Command	AS0 (value)	DriverLINX (value)
bipolar	bipolar	not supported	"yes" unipolar
unipolar	bipolar	not supported	"no"

Appendix E

Dimensions of Signals and Sensors' Sensitivity

To give the reader an idea about the relation between the signal strength and the sensitivity of the sensors and to enable him, to calculate the measurement-uncertainty or the quantization error, some number related to this topic are collected below:

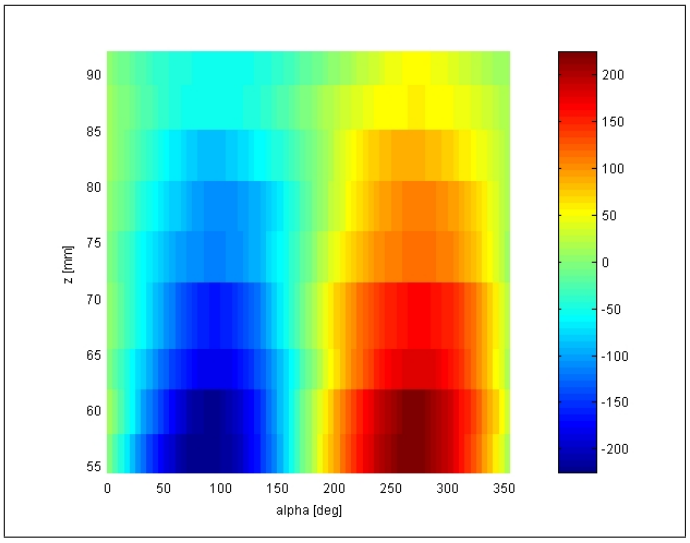

Figure E.1: Typical distribution of radial field component, by M. Ziolkowski

For bipolar signals, this means that the quantization interval is 20 V divided by 65536 states, giving approx. 0.305 mV. This is equivalent to about 16.5 nT or 24 (2*12.1) quantization intervals if the maximum signal is +/- 200 nT.
If the maximum gain (8) is used, this reduces to about 40 μV. With the output voltage factor of the sensors we find that this is equal to 2 nano Tesla.

Output voltage factor	18.5 $\frac{mV}{\mu T}$
measurement range	+/- 100 μT

Table E.1: Sensor sensitivity data

vertical	0 .. 100 nT
horizontal	0 .. 200 nT

Table E.2: Signal properties for 7.25 Hz, approx. 5 bar, Galinstan - 2molar KOH solution

vertical	0 .. 85 nT
horizontal	0 .. 10 .. 20 .. 150 nT

Table E.3: Signal properties from previous experiments (Cu-KOH, Mr. Men)

If the offset voltage allows to use unipolar signals, this value will halve.

From page 3-10 of the documentation:
"Screw terminal TB112 (+5V output) is current-limited through a series 10 Ohm resistor and allows a current up to 100mA. Note that you must take the voltage drop (current [I] multiplied by resistance [R]) across the series 10 Ohm resistor (1V at 100mA) into consideration."
Actually, the behavior of the power supply was found to be different

Resolution	16 bit
Input Range bipolar	+/- 10 V
Input Range unipolar	0 .. 10 V

Table E.4: Keithley Card resolution data, From Table A-1 in [KeithleyDoc].

Appendix F

Electrolyte

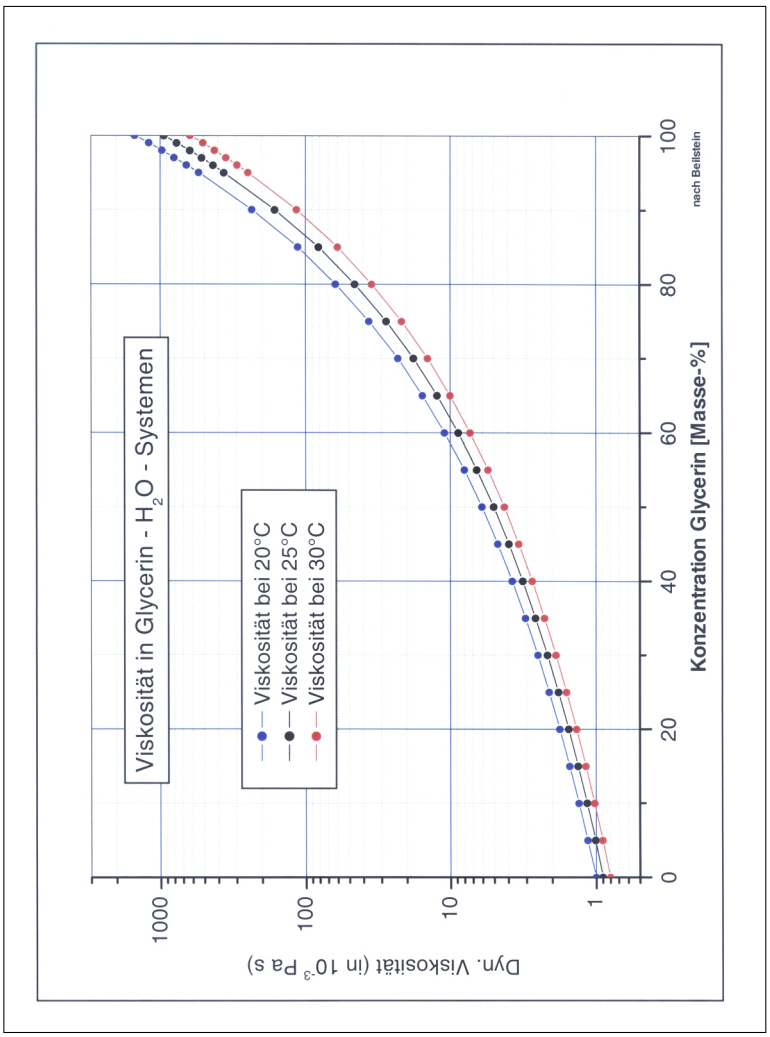

Figure F.1: Viscosity of a water-glycerol system, by FG Elektrochemie und Galvanotechnik, Data from Beilstein

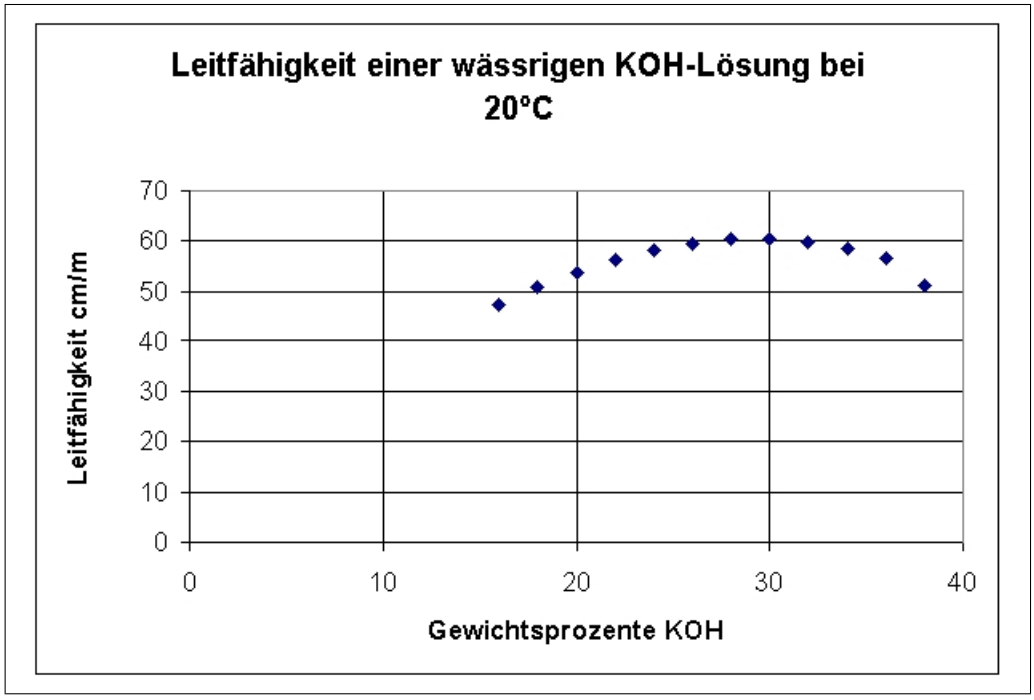

Figure F.2: Conductivity of an aqueous KOH solution

List of Figures

Bibliography

[Hope99] Kevin Hope
Measurement of the velocity fields and surface deformation of a two fluid system under the influence of mechanically generated vibrations
Project Work TU Ilmenau / University of Nottingham 1999

[Hackel] Tobias Hackel
Messung der Grenzflächendeformation in einem Zwei-Fluid-System unter Einwirkung von mechanischen Schwingungen
Studienarbeit TU Ilmenau

[Link02] Dietmar Link
Messung der Faraday-Oszillationen an der Grenzfläche zwischen zwei Flussigkeiten
Studienarbeit TU Ilmenau 2002

[Jung] Sascha Jung
Aufbau eines pneumatischen Schwingtisches
Studienarbeit TU Ilmenau

[Hauer02] Karl-Heinz Hauer
Entwicklung eines bildgebenden Messsystems, das es erlaubt, die räumliche Stromdichteverteilung in Brennstoffzellen nicht-invasiv zu erfassen
page 159-168
Sensoren und Mess-Systeme, VDE Verlag, 2002

[Resagk/Uhlmann04] Chr. Resagk, H. Uhlmann
Magnetfeldtomographische Detektion von Grenzflaechenbewegungen: Experiment und Sensorik
DFG Application 2004

[Vertesy] G. Vertesy, A. Gasparics, J. Szoelloesy
High Sensitivity Magnetic Field Sensor

[Resagk99] Chr. Resagk
Optische Charakterisierung von Gren-

zflächeninstabilitaeten in leitenden Fluessigkeiten
1999

[Men] Shouqiang Men et al.
Magnetic field measurement around a deformed interface

[Brauer03] H. Brauer et al.
Surface current reconstruction using magnetic field tomography
2003

[ThomäSievert04] E. Thomä, C.Sievert
Literaturrecherche
TU Ilmenau (internal paper)
2004

[PolytecManual] Polytec Vibrometer User's Manuals
Theory, Hardware, Software, Programming

[Seliger95] Hendrik Gunther Seliger
Laservibrometer, Erfassung mechanischer Schwingungen mit CO_2 Lasern
Verlag Shaker, Aachen
1995

[Baudisch] Olaf Baudisch
Aufbau und Erprobung einer elektrolytischen Zwei-Fluid-Messzelle zur Untersuchung von Grenzflächenschwingungen
TU Ilmenau
2004

[SieSch04] C.Sievert U. Schmidt
Experiment on gas production in electrolytes for the B1 experiment
TU Ilmenau (internal paper)
2004

[KeithleyDoc] Keithley Instruments Inc
KPCI 3116 user's manual
Revision C (January 2002)

[GaussmeterTET] Wuntronic GmbH
Bedienungsanleitung Koshava 3
München

[GaussmeterEW] Lake Shore Cryotronics, Inc
User's manual Model 421 Gaussmeter
Westerville, Ohio, USA
10 November 2000

[Video Manual] Canon Inc.
Digital Video Camcorder Instruction Manual
Japan
2001

[Wagner51] C. Wagner
Theoretical Analysis of the Current Density Distribution in Electrolytic Cells
Journal of the Electrochemical Society
page 116ff
1951

[KeithleySupport04] Keithley Inc.
othadcom.doc
Keithley Support Germany, Mr. Roland Blumberg
send by mail
16.07.2004

[Dobos75] D. Dobos
Electrochemical Data
Akademiai Kiado
Budapest
1975

[Heitz86] E. Heitz, G. Kreysa
Principles of Electrochemical Engineering
VCH
1986

[D'AnsLax49] J. D'Ans, E. Lax
Taschenbuch für Chemiker und Physiker
Springer
1949

[Davidson] P.A. Davidson
An introduction to magnetohydrodynamics
Cambridge University Press
2001

[Kuilekov] M. Kuilekov
Experimentalinvestigation

Internal report TU Ilmenau
2004

[Ziolkowski] M. Ziolkowski
Sent to Carsten pics.zip
Internal report TU Ilmenau
2004

Hiermit erkläre ich, dass ich die vorliegende Arbeit selbstständig durchgeführt und verfasst habe. Quellen, Literatur und Hilfsmittel, die von mir benutzt wurden, habe ich angegeben.

Carsten Sievert
Ilmenau, den 24.09.2004